





รายงานวิจัยฉบับสมบูรณ์

โครงการ Application of Multifunctional Reactors for C2

Hydrocarbons Production from Natural Gas
(การประยุกต์ใช้ปฏิกรณ์หลายหน้าที่สำหรับผลิตสารประกอบ
ไฮโดรคาร์บอน C2 จากแก๊สธรรมชาติ)

โดย ดร. วิศิษฏ์ศรี วิยะรัตน์ และ คณะ

ชันวาคม 2556

์สัญญาเลขที่ MRG5480185

รายงานวิจัยฉบับสมบูรณ์

โครงการ Application of Multifunctional Reactors for C2

Hydrocarbons Production from Natural Gas

(การประยุกต์ใช้ปฏิกรณ์หลายหน้าที่สำหรับผลิตสารประกอบ
ไฮโดรคาร์บอน C2 จากแก๊สธรรมชาติ)

ผู้วิจัย

สังกัด

ดร.วิศิษฏ์ศรี วิยะรัตน์ มหาวิทยาลัยเทคโนโลยีพระจอมเกล้าธนบุรี

ศาสตราจารย์ ดร. สุทธิชัย อัสสะบำรุงรัตน์ จุฬาลงกรณ์มหาวิทยาลัย

สนับสนุนโดยสำนักงานกองทุนสนับสนุนการวิจัย

(ความเห็นในรายงานนี้เป็นของผู้วิจัย สกว.ไม่จำเป็นต้องเห็นด้วยเสมอไป) Abstract

Project Code: 5480185

Project Title: Application of Multifunctional Reactors for C2 Hydrocarbons Production from

Natural Gas

Investigator: Dr. Wisitsree Wiyaratn

King Mongut's University of Technology Thonburi

E-mail Address: wisitsree@gmail.com, wisitsree.wiy@kmutt.ac.th

Project Period: 2 1 15 June 2011 – 14 June 2013

This project was aimed to develop new basic chemical and electrical cogeneration knowledge related

to solid oxide fuel cell reactor (SOFC) with novel Au/ LaSrMnO₃ nanocomposite, and Na₂WO₄-Mn

Experiments were carried out based on oxidative coupling of methane (OCM) in fixed bed reactor and

SOFC, which was designed for suitable C2 hydrocarbons production by promoting catalytic reaction of

OCM. The study is divided into 2 parts: 1) oxidative coupling of methane (OCM) in fixed bed reactor

and SOFC reactor over Au/ LaSrMnO₃ nanocomposite and Na₂WO₄-Mn. From the works, 1

international paper have been accepted for publication, and 1 paper was presented in international

conferences.

Keywords: Au/ LaSrMnO₃, Na₂WO₄-Mn, SOFC reactor ,Oxidative coupling of

Methane, Chemical and electrical cogeneration

บทคัดย่อ

รหัสโครงการ: MRG 5480185

ชื่อโครงการ: การประยุกต์ใช้ปฏิกรณ์ หลายหน้าที่สำหรับผลิตสารประกอบไฮโดรคาร์บอน C2 จาก แก๊สธรรมชาติ

ชื่อนักวิจัย: ดร. วิศิษฏ์ศรี วิยะรัตน์ มหาวิทยาลัยเทคโนโลยีพระจอมเกล้าธนบุรี

E-mail Address: wisitsree.wiy@kmutt.ac.th

ระยะเวลาโครงการ: 16 มีนาคม 2552 – 15 มีนาคม 2554

งานวิจัยนี้มีวัตถุประสงค์เพื่อสร้างองค์ความรู้พื้นฐานของการร่วมผลิตสารเคมีและกระแสไฟฟ้าที่เกี่ยวข้องกับ เครื่องปฏิกรณ์แบบเซลล์เชื้อเพลิงแข็ง ร่วมกับตัวเร่งปฏิกิริยา Au/LSM นาโนคอมโพสิ ผ่านปฏิกิริยาคู่ควบของ มีเทนแบบออกซิเดชันในปฏิกรณ์เบดนิ่งและปฏิกรณ์แบบเซลล์เชื้อเพลิงแข็ง งานที่ศึกษาสามารถแบ่งออกได้ เป็น 2 หัวข้อย่อย คือ 1) การสังเคราะห์ตัวเร่งปฏิกิริยาและวิเคราะห์โครงสร้าง 2) การศึกษาปฏิกิริยาคู่ควบของ มีเทนแบบออกซิเดชันในปฏิกรณ์เบดนิ่งและเครื่องปฏิกรณ์แบบเซลล์เชื้อเพลิงแข็ง ผลงานที่ได้จากการศึกษานี้ คือ บทความที่นำเสนอในระดับนานาชาติ จำนวน 1 บทความ และการนำเสนอผลงานในที่ประชุมระดับ นานาชาติ จำนวน 1 บทความ

คำหลัก: เครื่องปฏิกรณ์แบบเซลล์เชื้อเพลิงแข็ง, Au/ LaSrMnO₃ นาโนคอมโพสิต, ปฏิกิริยาคู่ควบของมีเทนแบบออกซิเดชัน, การร่วมผลิตสารเคมีและกระแสไฟฟ้า

CHAPTER 1

INTRODUCTION

1.1 Rationale

A solid oxide fuel cell (SOFC) is an electrochemical device that produces electricity directly from a fuel. The advantages of SOFCs include high system efficiency, fuel flexibility and low emissions. Most SOFC studies are aimed at only electricity generation, during which the fuels are completely combusted to CO₂ and H₂O. However, there has been some research focusing on applications of SOFCs for the cogeneration of chemicals and electrical power. Various reaction systems have been tested, including styrene production from ethylbenzene [1], partial oxidation of methane (POM) to synthesis gas [2-4] and oxidative coupling of methane (OCM) to C2 hydrocarbons (ethane and ethylene) [5]. The effective catalytic conversion of methane into more useful and valuable products (such as H₂, syngas and C2 hydrocarbons) with sufficiently high yields, selectivity and stability remains a great challenge. Generally, SOFCs operate at 800-1000°C, so materials with high activity and stability at high temperatures are necessary [6-8]. The search for new anode catalysts aims to improve the conversion, selectivity, yield and stability.

In the search for catalysts affording catalytic reactions in SOFCs, perovskite oxide precursors are good candidates. This is because perovskite oxide systems have stability over a broad temperature range as well as a high oxygen storage capacity and oxygen ion conductivity [9-12]. Perovskite oxides are versatile for many catalytic reactions, including the oxidation of hydrocarbons. Doped noble metals (Pt, Pd, Rh) over a perovskite support lead to ameliorated catalyst performance in terms of activity and stability at high operation temperatures. Rh-LaCoO₃/Al₂O₃ and Rh/LaMnO₃/Al₂O₃ [3] have been employed in syngas generation. In particular, doped nanoparticles,

such as Au over a metal oxide support, can promote catalytic activity because the catalytic performance is significantly affected by the size of the particles and the distribution [13-16]. Metal oxides as ultra-fine particle supports promote changes in the chemistry of noble metals [17-21]. Au/LaSrMnO₃ and LaSrCrO₃ perovskite composite catalysts have been investigated as potential anode catalysts in SOFCs for propane reforming processes [8]. Au/LaSrMnO₃ showed a higher activity for propane reforming than Au/LaSrCrO₃.

Among several catalysts, 5wt%Na₂WO₄-2wt%Mn/SiO₂ offers a good performance in OCM with 20% of methane conversion and 80% of C2+ selectivity [22, 23-25]. Lunsford and co-workers reported that Na-O-Mn species are responsible for an activation of methane, in which Mn is an active component, Na provides selectivity, and W is required to stabilize the catalyst [26, 27]. Afterwards, Lapeña-Rey et al. investigated OCM in SOFC using YSZ as a solid electrolyte, 5wt%Na2WO4-2wt%Mn/SiO₂ was used as an anode catalyst. Very high C2 hydrocarbon selectivity was found while the methane conversion was low. However, the SiO₂ support has low electrical conductivity, thus it was required to be mixed with a conductive component such as silver to increase the electrical conductivity [28]. From the disadvantages of SiO₂ support, a new support is desirable for increasing the electrical conductivity and catalytic properties of the anode in SOFC. YSZ is considered a good candidate because it is used to match the thermal expansion coefficient of the anode to be close to that of the YSZ electrolyte and provides an ionic pathway for conveying oxygen ions from the electrolyte to the three-phase boundary. The main objective of this research was to investigate the new anode catalysts in SOFC. Au/ LaSrMnO₃, and 5wt%Na₂WO₄-2wt%Mn/YSZ catalysts were examined. The surface morphology, composition and surface area were characterised using several techniques. The catalytic activity of catalysts for OCM was evaluated using a continuous-flow fixed bed reactor and SOFC reactor.

.

1.2 Research Objectives

The aim of this research work is to study the potential use of Au/ $La_{1-x}Sr_xMnO3$ (x ≈ 0.4) perovskite materials , and 5wt%Na₂WO₄-2wt%Mn/YSZ for the oxidative coupling of methane reaction in SOFC reactor to co-generate C2 hydrocarbons and electrical power.

1.3 Scope of Research Work

 $La_{1-x}Sr_xMnO_3$ (x ≈ 0.4) and 5wt%Na₂WO₄-2wt%Mn/YSZ was selected as perovskite-based material because it has widely been reported to enhance good activity for the oxidative coupling of methane (OCM) reaction. Those materials were then characterized their properties such as total surface area and pore size, phase formation, morphology, and elemental analysis. Then, the prepared materials were evaluated the catalytic activities on OCM. The investigated parameter consisted of temperature, $CH_4:O_2$ ratio, $CH_4:O_2$ ratio and temperature. The results were presented in term of percent conversion of methane, product selectivity, and product yield (especially in C_2 hydrocarbon product).

1.4 Research Planning

To achieve the research objectives and research scope, the research methodology will be provided as,

- To review literatures on related topics, i.e. OCM, SOFC
- To prepare La_{1-x}Sr_xMnO₃ (x ≈ 0.4) and 5wt%Na₂WO₄-2wt%Mn/YSZ
- To investigate the performance of catalysts in oxidative coupling of methane reaction by fixed-bed reactor.
- To study OCM reaction in SOFC.
- Analyze the obtained data to find the conclusion of the research.

•

CHAPTER 2

THEORIES

Among various types of fuel cell, SOFCs are one of the most promising fuel cell due to efficient operation with diversity range of fuels. As a result, SOFCs have been the object of intensive R&D (research and development). The important issues for developing of SOFCs are construction materials and co-generation of chemical Production. Therefore, this chapter describes main topics that relate to this research such as solid oxide fuel cells (SOFCs) technology, fuel cells reactors, principle of cogeneration of chemical production, perovskite materials, principle of catalyst, and synthesis of solid catalysts, and principle of oxidative coupling methane (OCM).

2.1 Fuel cells

The production of chemicals and energy that provide high efficiency and non pollutant to environmental is a final destination for energy technologies and chemical reactors development that will soon help to sustainable development in the world. At the foreground of energy technologies, fuel cells (FCs) are expecting to find various applications in the direct convertibility of chemical reactions into electrical energy with high efficiency and small pollutant since they generate much less pollutants than combustion process.

Group of fuel cells can be divided to their electrolyte employed or working temperature (high, moderate and low temperature, etc.) For example, alkaline fuel cell (AFC), proton exchange membrane fuel cell (PEMFC), phosphoric acid fuel cell (PAFC) operates at low temperatures and aqueous electrolyte can be used. The molten carbonate fuel cell (MCFC) and solid oxide fuel cell (SOFC) operate at high temperature with molten electrolyte and solid electrolyte, respectively. Table

2.1 shows different types of fuel cells, distributed to the electrolyte employed, and working temperature [29-37].

Table 2.1 Group of fuel cells divided to electrolyte and temperature functionalized

	AFC	PEMFC	PAFC	MCFC	SOFC
Temperatur e (°C)	60-90	80-110	160-200	600-800	800-1000
Electrode material	Metal or carbon	Pt-on carbon	Pt-on-carbon	Ni+Cr	Ni/Y ₂ O ₃ - ZrO ₂
Electrolyte	NaOH/KO H	Polymer membrane	H ₃ PO ₄	LiCO ₃ - K ₂ CO ₃	ZrO ₂ with
Primary fuel	H ₂	H ₂ reformate	H ₂ reformate	H ₂ /CO reformate	H ₂ /CO/CH ₄ reformate
Oxidant	O ₂ /air	O ₂ /air	O ₂ /air	CO ₂ /O ₂ /air	O ₂ /air
Issues	CO ₂ troubles	Moisture of fuel	CO sensitivity	CO ₂ recycling necessary	Ceramic cells
Practical efficiency (%)	60	60	55	55-65 ^a	60-65 ^a

^a The production of additional electrical energy by means of thermal energy co-generation is not concerned [31].

2.2 Principle of Fuel Cells

A principle of FCs system composes an electrolyte solution and porous electrode e.g. anode and cathode electrode on either side. The typical fuel cell, gaseous fuels (i.e. hydrogen) are supplied continuously to the anode electrode (negative electrode) and an oxidant (i.e., oxygen from air) is fed continuously to the cathode electrode (positive electrode); the electrochemical reactions suddenly occur at the electrodes surface and produce electricity with the by-products including heat and water. The reactions are shown below.

Anode:
$$2H_2 \rightarrow 4H^+ + 4e^-$$
 (1)

Cathode:
$$O_2 + 4H^+ + 4e^- \rightarrow 2H_2O$$
 (2)

OverallCellReaction:
$$2H_2 + O_2 \rightarrow 2H_2O$$
 (3)

The overall efficiency of FCs is about twice higher than internal combustion engines and other methods of electricity production from the equal amount of fuel. The following lists summarize the most important features of FCs in comparison to other energy conversion devices [29,31,32]:

- FCs are power generators which are able to directly change chemical energy of fuel (hydrogen, methane, naphtha, etc.) into electrical energy which the efficiency is higher than conventional coal or gas fired thermal power stations (35-40%).
- If the waste heat of fuel cell is used in system, the fuel efficiencies are possible to go up 90%.
- Low pollution level emissions are produced from FCs (typically one to two orders of magnitude lower).
- Low noise level is generated.
- FCs require low maintenance and exchangeable parts (mass-produced components).

- The efficiency of FCs can be increased by applying the cogeneration of heat with high-temperature systems.
- For cogeneration of high temperature, waste heat is useful for many applications such as industrial processes or for additional electricity production.

2.2.1 Cell Components and Materials for SOFC

The major components of an individual SOFC include the electrolyte, the cathode, and the anode. Fuel cell stacks contain an electrical interconnect which links individual cells together in series or parallel. The objective of this system is to generate more power. These fuel cell components involve with the development of SOFC performance. The SOFC performance, that should be enhanced, consists of higher energy conversion efficiency, lower chemical and acoustical pollution, fuel flexibility, cogeneration capability, and a rapid load response.

Figure 2.1 illustrates the structure and properties of the SOFC components. The SOFC employs a solid oxide ceramics as the electrolyte, which is the main component of SOFC. The electrolyte is an oxygen ion (oxygen vacancy) conductor. The cathode electrode, similarly as the anode electrode, should be an ion-electronic conductor. However, the anode and cathode materials in a SOFC are different. The fuel electrode must be able to withstand the highly reducing high-temperature environment of the anode, while the air electrode must be able to withstand the highly oxidizing high-temperature environment of the cathode [38]. Another part of SOFC such interconnect of fuel cell stacks to conduct the electron through an external circuit. The structure of cathode and anode materials should be porous, in order to allow the penetration of gases. In the layers close to the electrolyte, however, the porosity should be as low as possible to intensify the lattice diffusion of oxygen. The electrolyte is a gastight sinter with high strength, preventing a non-productive combustion of the fuel [39]. The important issues of the cell components are chemically and thermally compatible.

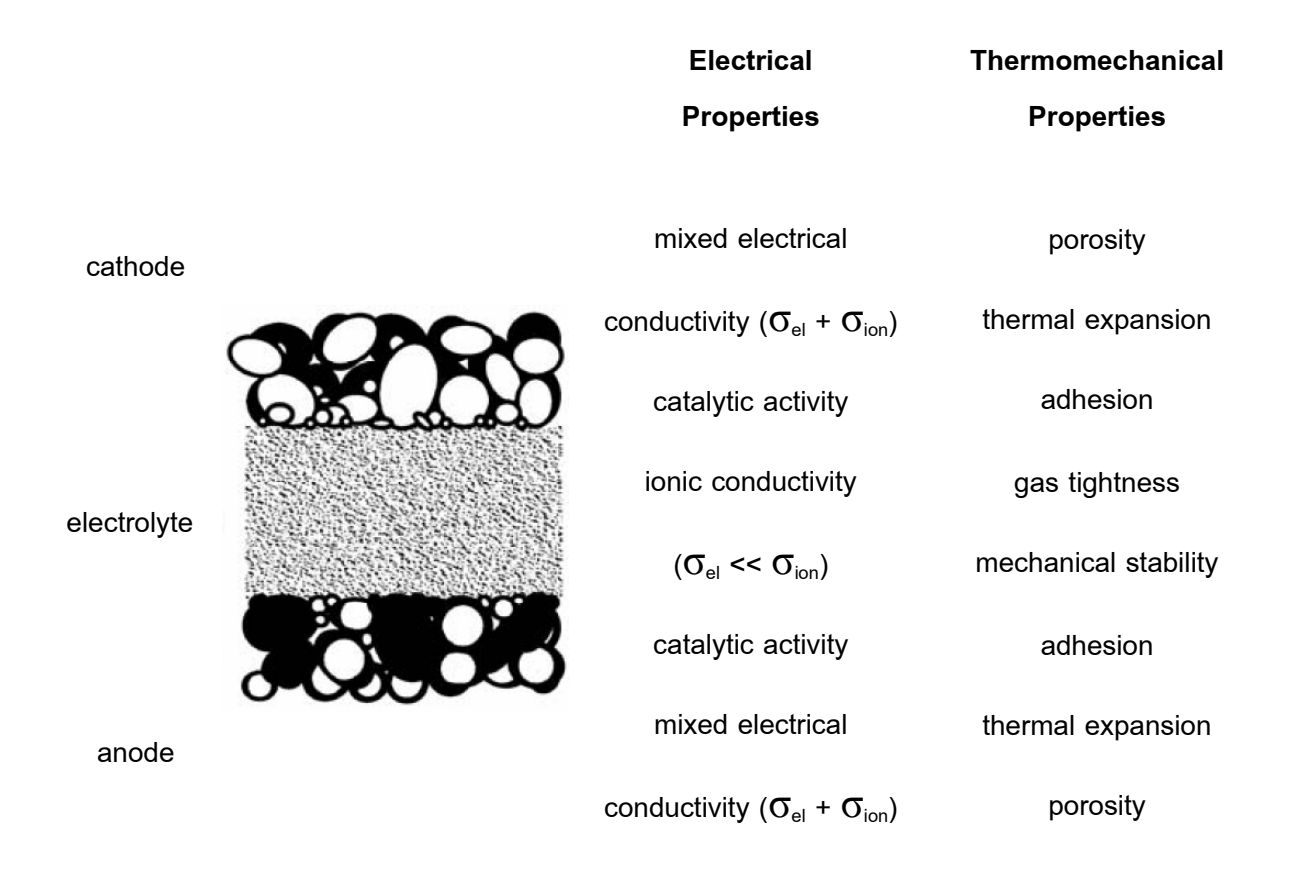


Figure 2.1 Schematic cross-section of SOFC components [32].

a) Electrolyte Materials

The typical challenges of SOFC electrolyte development consist of matching the thermal expansion coefficients, mechanical strength, and chemical compatibilities. Several solid oxide ceramics, typically perovskites (structure ABO₃), have been tested as SOFC electrolyte. Yttria-stabilized-zirconia (YSZ); 3, 8 or 10 percent yttria, is the most commonly used for SOFC electrolyte material. YSZ electrolyte provides high conductivity at temperatures above 700°C, while exhibiting negligible electronic conductivity at these temperatures.

Alternative electrolytes have been considered and are being developed. The interested electrolyte materials are scandium-doped zirconia (SDZ), gadolinium-doped ceria (GDC), and perovskite-based lanthanum gallate (LaGaO₃).

b) Cathode Materials

EG&G Technical Services (2004) [40] reported that during early development, platinum and other noble metals, and even magnetite, were used as cathode materials for SOFC. They are no longer pursued actively because of chemical and physical instability, incompatibility with most electrolytes, and cost (in the case of platinum). Currently, materials used in SOFC cathode are lanthanum-based perovskite materials. These materials are considered as good oxidation resistance and high catalytic activity in the cathode environment. The most cathodes are based on doped lanthanum manganites (LaMnO₃). In high operating temperature SOFC (~1,000°C), strontium-doped LaMnO₃ (LSM) is used.

c) Anode Materials

The composition of the anode material, particle sizes of the powders, and the manufacturing method are key to achieving high electrical conductivity, adequate ionic conductivity, and high activity for electrochemical reactions and reforming and shift reactions [40]. In addition, the SOFC anode that will be operated with hydrocarbon fuels should look first at materials.

Anode materials for SOFC have been considered in wide range of materials. Early stage of SOFC development, precious metals such as platinum and gold were used, as well as pure transition metals such as nickel and iron. Subsequently, other materials such as nickel aluminide were tested because of the physical and chemical instability of these materials.

The most common material for the anode electrode is a nickel-YSZ cermet (a cermet is a mixture of ceramic and metal). The ionic conductivity is associated with oxygen ion transport via oxygen vacancies in YSZ. The presence of metallic nickel in the anode material provides the

electronic conductivity and catalytic activity by catalyze the fuel oxidation. As for the YSZ provides ion conductivity, other properties such as thermal expansion compatibility, and mechanical stability, and maintain the high porosity and surface area of the anode structure is also provided by YSZ. The main degradation of Ni-YSZ cermet is the morphology (i.e. size and shape) changing from the sintering. Moreover, the catalytic activity of Ni-YSZ could be destroyed from the carbon deposition when hydrocarbon fuels are used for SOFC operation.

McIntosh and Gorte (2004) [41] mentioned about ceramic anodes that the provskite materials have possibility for the application of SOFC anode. The perovskite must be capable of catalyzing the hydrocarbon oxidation reactions while maintaining high electronic conductivity and structural stability in the highly reducing environment. Various perovskites have been investigated the stability for SOFC application. For example, materials based on doped LSM, LaCrO₃ were reported to be quite stable. Depending on the dopant, degradation can occur due to reaction with YSZ, due to reduction of the oxide, or due to electrochemical demixing; however, it was reported that, for this material, degradation can be slow even when the oxide is thermodynamically unstable.

The catalytic activities of some perovskites for methane oxidation and steam reforming have also been studied, and it appears that the activity of some materials can be reasonably attractive. Materials based on LSM, Au/LSM, steam reforming and methane oxidative-coupling activities have been shown to depend strongly on the dopant ion. Materials doped with Au gave particularly high steam-reforming activities with lower propensity for carbon formation as compared to a normal Ni catalyst.

d) Interconnect Materials

The interconnect of SOFC is the electric link to the cathode and protects the electrolyte from the reducing reaction. Therefore, the interconnect must be an electronic conductor and have similar characteristics to the electrolyte. Broadly, interconnect materials for SOFC can be divided into two categories: conductive ceramic (perovskite) materials for operation at high temperature (900 to 1,000 °C) and metallic alloys for lower temperature operation.

2.3 Fuel Cells Reactor

As mentioned above, fuel cell is usually used as a power generator but it can be also applied as a chemical reactor. Previously, fuel cell reactors have been developed for the conversion of fuel to desired chemicals as the main product with energy generation [31] that is called chemicals and energy co-generation. In this process, the main function of fuel cell likes chemical reactor. However, electricity generated as by-product from the fuel cell reactor distinguishes it from the conventional reactor. In addition, chemicals and energy co-generation provides a benefit over a conventional fuel cell which just produces electrical and pure water as a by-product.

The typical concept of fuel cell reactor for chemicals and electrical power co-generation is illustrated in Figure 2.2. This system consists of fuel cell reactor, external load and chemical product recovery unit [31]. The fuel and oxidant are supplied separately to electrochemical cell (anode and cathode electrode) at fuel cell reactor, after that useful chemical and electricity are occurred. Electricity is supplied to an external load and useful chemical produced is collected. Cogeneration systems can operate at low, moderate or high temperatures; hence the electro-cogeneration process has become one of the new applications for fuel cell system.

The main advantages of the chemical and energy co-generation methods over the conventional catalytic reactors (batch reactor, plug flow reactor, continuous stirred tank reactor, etc.) are as follows [29,31,32]:

- The cell potential mainly controls the production in the electrochemical reactor.
- -The selectivity of chemical production can be controlled by difference of the electrode potential or changing the electrode catalyst.
- -The electrochemical devices can operate at very low temperatures when compare to conventional catalytic processes.
- -Co-generation of electricity and useful chemical products is efficient which improve the potential of industries.
- -Successful chemical cogeneration has been controlled by suitable selection of anode material and the fuel.

Therefore, fuel cell reactors for co-generation of chemicals-electrical power have become an attractive new application for fuel cell system. Many co-generation processes with different types of FCs have been discussed. Selective electrochemical oxidations of methane to synthesis gas or C2 compound with electricity in SOFC reactors are a very attractive alternative to conventional catalytic reactor. Hydrogen peroxide (H₂O₂) can be produced in an AFC reactor. PEMFC reactors show the ability to convert fuel to useful chemicals such as 1- propanol, H₂O₂, and cyclohexlamine (CHA). It is noted that this review will focus mainly on chemical and electrical power co-generation by fuel cell reactor and describes their reactions and performances.

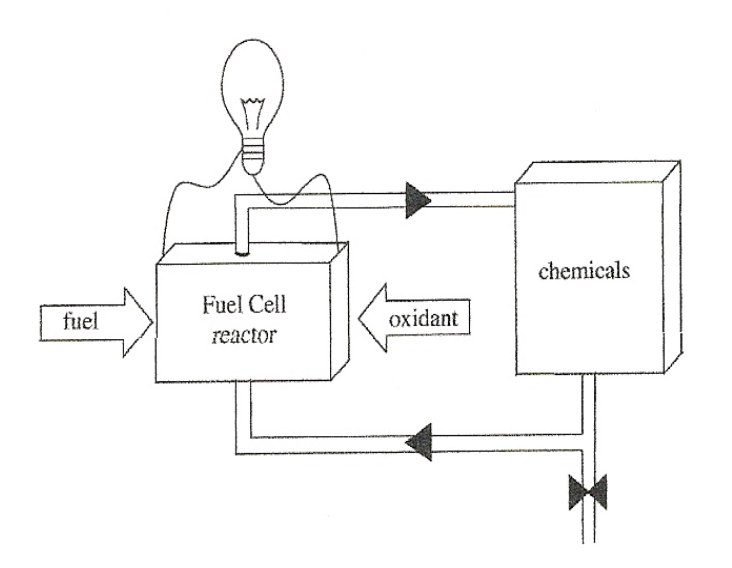


Figure 2.2 Principle fuel cell reactor to generate chemical and electricity [31].

2.4. Co-generation of Fuel Cell: Chemical Production

2.4.1 Co-generation of SOFC Reactor

Farr and Vayenas [42] first demonstrated this type of operation for the case of NH₃ conversion to NO. They studied the nitric oxide production from oxidation reaction of ammonia and obtained electricity as by product. The result showed that, NO was obtained as a primary product with an optimal yield of over 60% when the temperature ranges from 427 to 927°C. Another interesting chemical co-generation process is the synthesis of hydrogen cyanide (HCN), which is widely used for adiponitrile (for Nylon 6/6) synthesis [43]. The selectivity of HCN exceeds 75% and approximately 0.01 W cm⁻² of power density was obtained in the temperature range 800 to 1000°C and 1 atm [44].

Occurring of organic compounds e.g. styrene can be studied by electrochemical oxidation of ethylbenzene dehydrogenation in SOFC. The vapor-phase electrochemical oxidative dehydrogenation of ethylbenzene on platinum-paste electrodes was studied at 575–600°C in a stabilized-zirconia electrochemical reactor. Styrene and carbon dioxide were the major products. Nevertheless, increasing in a dehydrogenation rate occur in high anodic current, total conversion was limited at only 15% or less [45].

$$C_6H_5 - CH_2CH_3(g) + O^{2-} \rightarrow C_6H_5 - CH = CH_2(g) + H_2O(g) + 2e^-$$
 (4)

$$2CH_4(g) + 2NH_3(g) + 3O_2(g) \rightarrow 2HCN(g) + 6H_2O(g)$$
 (5)

Another interesting chemical cogeneration process is the synthesis of Acrylic acid in SOFC. A highly efficient anode catalyst, $MoV_{0.3}Te_{0.17}Nb_{0.12}O$, was used for acrylic acid production from propane [46]. The partial oxidation of methanol to formaldehyde, which is an important compound for fertilizer, dyes, disinfectants, germicides and preservatives, is another important industrial reaction that has been reproduced successfully in SOFC [47]. From that work, methanol conversion was over 30%, with formaldehyde selectivity 85–92% and power density outputs obtained of about 1mW cm⁻².

The oxidation reaction of H_2S to SO_2 has also been successfully demonstrated [48]. At 650–800 C and atmospheric pressure, hydrogen sulfide was oxidized on the porous Pt electrode. Hydrogen sulfide was diluted in He and used as fuel, while ambient air was used as oxidant. Reaction (6) presents the anode reaction, whereas the cathode reaction is similar to Reaction (5). Reaction (7) is the overall reaction of this system.

$$2H_2S(g) + 3O^{2-} \rightarrow SO_2(g) + 2H_2O(g) + 6e^-$$
 (6)

$$2H_2S(g) + 3O_2(g) \rightarrow 2SO_2(g) + 2H_2O(g)$$
 (7)

From their experiment, the selectivity to SO_2 remained under 15% is observed at low current densities (<10 mA cm⁻²) and sulfur, (1/2) S_2 (g), is the main product. Nevertheless, at high current densities (>40 mA cm⁻²), the SO_2 selectivity increased above 90%.

Selective oxidation of methane in SOFC was studied for co-generation of C2 hydrocarbons or synthesis gas. As for the conversion of methane, typically, the oxidative coupling of methane has been studied mostly in conventional reactors [49-53]. Nevertheless, there have been few studies apply SOFC for the direct conversion of methane to useful chemicals. For instance, Solid oxide fuel cell system with membrane reactor is investigated, which anode electrode is LaAlO and cathode is LSM.

When electrochemical reaction occurred, oxygen ion transferred from cathode cell to anode cell by equation (8) and (9).

Cathode:
$$O_2 + 4e^- \rightarrow 2O_2^-$$
 (8)

Anode:
$$CH_4 + 2O_2^- \rightarrow 2C_2H_4 + H_2O + 4e^-$$
 (9)

In the reaction, it could produce valuable chemicals such as ethylene and carbon monoxide with high selectivity and provided electric power with high efficiency.

Pujare and Sammells [54] investigated the oxidative coupling of methane with SOFC. High C_2 hydrocarbon selectivity (> 90%) was observed, although the methane conversion was relatively low. Otsuka et al. [55] also investigated similar studies over several catalysts (i.e. KF, BaCO₃, NaCl/MnO₂, Sm₂O₃) deposited on Au-electrode. The result showed that BaCO₃ on Au was the most active and selective catalyst. Jiang et al. [49] investigated the oxidative coupling of methane to ethylene and C_2 hydrocarbons and the yield values above 88% with 97% of the methane conversion at 800 C was observed. In their work, anodes were porous Ag film and Sm₂O porous cermet , which modified with CaO and Ag. Eqs. (10) and (11) present the anode and overall reactions of the above system.

$$2CH_4(g) + 2O^{2-}(g) \rightarrow C_2H_4(g) + 2H_2O(g) + 4e^-$$
 (10)

$$2CH_4(g) + O_2(g) \rightarrow C_2H_4(g) + 2H_2O(g)$$
 (11)

Guo et al. [57] investigated SOFC with Sr/La₂O₃-Bi₂O₃-Ag-YSZ membrane for oxidative coupling of methane and revealed that composition of membrane showed a important effect on the cogeneration. The stability of membrane was continuously investigated for 62 h and no activity obviously declined (C₂-selectivity and CH₄ conversion showed relatively stable). Kiatkittipong et al. [30,58]

investigated solid oxide fuel cell reactor using $La_{0.85}Sr_{0.15}MnO_3/8$ mol% Y_2O_3 - $ZrO_2/La_{1.8}Al_{0.2}O_3$ for C_2 hydrocarbon production. The most of C_2 production is ethylene, which is more favored than ethane. However, the influence of increasing methane flow rate effected to the decreasing methane conversion while C_2 selectivity slightly increases.

Syngas and electrical power in direct-methane solid oxide fuel cell (SOFC) was reported [59-65]. Syngas can be used as feedstock for hydrocarbon and methanol manufacture. The syngas cogeneration enhanced when increasing bulk lattice-oxygen extraction from electrochemical reaction [63-69]. This observation occurred when providing external potential to the electrochemical cell, ionic species migrated to the electrode surface and makes the changing the operation of catalysts electrode, which corresponded to a change in activation energy and the rate of catalytic reaction. This observation can be applied to supply methane in a period for the synthesis gas and electricity production, in which electrical current is obtained when fed methane just one fifth of overall working time [68].

Ishihara et al. [70] studied the co-producing of syngas and electricity by SOFC. Partial oxidation of methane $CH_4+1/2O_2=CO+2H_2$ as internal reforming reaction was investigated. From their study, the maximum power density of 526 mW cm $^{-2}$ with synthesis gas yield of 20% can be achieved. Similar investigation was performed by Pillai et al. [71]. They reported that, SOFC produced 0.9 Wcm $^{-2}$ and methane was converted to syngas with 90 % of methane conversion at a rate of 30 sccm cm $^{-2}$, 750 °C.

The possibility of synthesis gas and electricity production from electrochemical partial oxidation of CH₄ in SOFC has been studied by numerical simulation. In catalytic reaction of CH₄, energy occurring in the partial oxidation reaction at perovskite cathodic electrode can be supplied in flow reversal operation in SOFC. Thermodynamic efficiency occurred in the reaction showed exceeding

unity (η > 2), which revealed the interesting in the SOFCs to produce valuable chemicals and electrical energy [72].

According to economic analysis of SOFC for chemical cogeneration, until now, very limited works have been reported. Brousas et al. [73] designed SOFC plant for complete oxidation of methane to CO_2 and H_2O while another SOFC plant was aimed for synthesis gas and electricity. They evaluated these systems and were found that the synthesis gas was low. Therefore, SOFC plant coproducing synthesis gas has so far to expand to large-scale application. Vayenas et al. [74] proposed the index for evaluating the relative profitability of SOFC chemical co-generation compared to the chemical reactor at same product capacity and composition. Only SOFC reactor using inexpensive material with exothermic reaction might be beneficial. The results showed that H_2SO_4 and HNO_3 cogeneration were possibly advantageous while ethylene oxide and formaldehyde production were not.

2.5 Perovskite Materials

2.5.1 General Characteristics of Perovskites as Catalysts

There are many compounds in the perovskite such as oxides, carbides, nitrides, halides, and hydrides that crystallize in this structure. The most interesting perovskite is perovskite-type oxide that has the general formula ABO₃ (A is a larger cation than B). The board diversity of perovskite properties is from the synthesis of multicomponent perovskites by partial substitution of cations in positions A and B. The perovskite structure can tolerate significant partial substitution and non-stoichiometry; for example, metal ions having different valences can replace both A and B ions. Because of their varied structure and composition, perovskite materials have attracted intense interest in many applied and fundamental areas of solid state chemistry, physics, advanced materials, and catalysis [75]. A partial list of their potential applications is presented in Table 2.2.

Table 2.2 Applications of perovskites in materials [75].

Multilayer Capacitor	BaTiO ₃	
Piezoelectric Transducer	Pb (Zr, Ti) O ₃	
P. T. C. Thermistor	BaTiO ₃ , doped	
Electrooptical Modulator	(Pb, La) (Zr, Ti) O ₃	
Switch	LiNbO ₃	
Dielectric Resonator	BaZrO ₃	
Thick Film Resistor	BaRuO ₃	
Electrostrictive Actuator	Pb (Mg, Nb) O ₃	
Superconductor	Ba (Pb, Bi) O ₃ Layered cuprates	
Magnetic Bubble Memory	GdFeO ₃	
Laser Host	YAIO ₃	
Ferromagnet	(Ca, La) MnO ₃	
Refractory Electrode	LaCoO ₃	
Second Harmonic Generator	KNbO ₃	

2.5.2 Structure of Perovskites

a) Crystal Structure [41,76]

The ideal perovskite-type structure is cubic with the unit formula of perovskite-type oxide ABO₃. A and B in the perovskite structure are cations with a total charge of +6. The lower valence A cations are larger and reside on the six-fold coordinated corners of a simple cubic lattice, with the B cations occupying the twelve-fold coordinated center site. The oxygen atoms are found in a face

centered structure around the central B cation. The unit cell of ABO₃ perovskite structure is shown in Figure 2.3. In that structure, A ions can be alkali, alkaline earth, rare earth, and other large ions, while B ions can be 3d, 4d and 5d transitional metal ion.

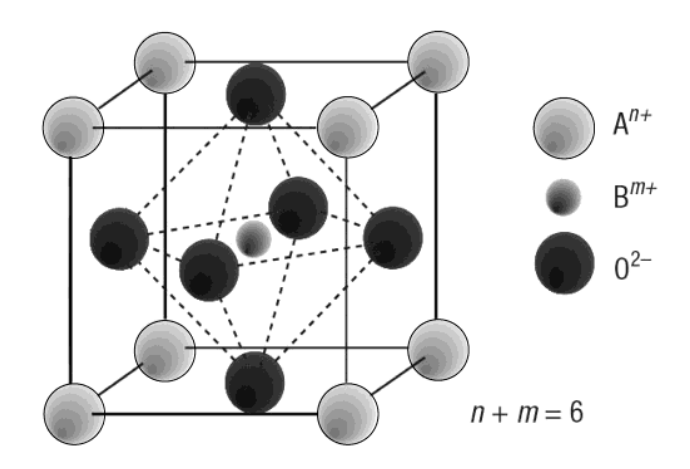


Figure 2.3 Unit cell of ABO₃ perovskite structure [41].

In the ideal perovskite structure, where the atoms are touching one another, the B-O distance is equal to a/2 (a is the cubic unit cell parameter) while the A-O distance is $(a/\sqrt{2})$ and the following relationship between the ionic radii holds: $(r_{\rm B}+r_{\rm O})=\sqrt{2}(r_{\rm B}+r_{\rm O})$. However, it was found that the cubic structure was still retained in ABO₃ compounds, even though this equation is not exactly obeyed. As a measure of the deviation from the ideal situation, Goldschmidt introduced a tolerance factor (t), defined by the equation:

$$t = \frac{(r_{\rm A} + r_{\rm O})}{\sqrt{2}(r_{\rm B} + r_{\rm O})}$$
 (12)

where r is the ionic radius of A,B, or oxide ion.

This equation is applicable at room temperature to the empirical ionic radii. Although for an ideal perovskite t is unity, this structure is also found for lower t-values (0.75 < t < 1.0). The ideal cubic perovskite structure appears in a few cases for t-values very close to 1 and at high temperatures. In most cases, different distortions of the perovskite structure appear. The naturally occurring compound CaTiO₃ was originally thought to be cubic, but its true symmetry was later shown to be orthorhombic.

The perovskite structure is stable to relatively large amounts of dopant ions on either A or B sites. Oxygen vacancies are introduced into the lattice, either through transition-metal redox processes or by doping on the A or B sites with lower valence cations. Doping of the lattice can alter the structural stability, catalytic activity, and ionic and electronic conductivities of the perovskite. For example, at oxygen contents just below stoichiometry, A-site doped perovskites of the form La₁. $_x$ Sr $_x$ FeO $_3$ show p-type conductivity. This is due to the Sr-induced charge deficiency being balanced by oxygen vacancies, and relative to the neutral lattice, positively charged Fe ions. At low oxygen activity, the mechanism is n-type as the Fe ions are reduced.

Deviations from the ideal structure with orthorhombic, rhombohedral, tetragonal, monoclinic, and triclinic symmetry are known, although the latter three ones are scarce and poorly characterized. The distorted structure may exist at room temperature, but it transforms to the cubic structure at high temperature. This transition may occur in several steps through intermediate distorted phases. These deviations from the cubic perovskite structure may proceed from a simple distortion of the cubic unit cell, or an enlargement of the cubic unit cell, or a combination of both.

2.6 Catalyst Properties

The physical and chemical properties of the catalyst represent the performance of that catalyst. An excellent performance such as high surface area and high activity are required for good catalyst. The properties of good catalyst can be determined as following items.

a) Size

Size of catalyst is one of the important parameter to consider the performance of the catalyst.

The small size of catalyst provides high surface area and gives better catalytic performance.

b) Surface Area

High surface area is usually desirable for high activity per unit volume or unit weight. Consequently, most catalysts are made to be porous, with high internal surface area about 1000 m²·g⁻¹. The porous structure and pore size distribution of the catalyst may cause diffusion resistance that affect the access of reactant to the catalyst sites and removal of the product. Therefore, they also affect the rate and selectivity of the reaction. For very fast reaction, a large pore size (low surface area) catalyst may be desired

c) Stability

This includes stability of heat, to poisons, to fluctuations in process conditions, and to such common component of the reacting mixtures.

d) Activity

The activity of the catalyst refers to the rate at which it causes the reaction to proceed to chemical equilibrium. The rate of reaction depends on temperature, pressure and concentration of reactant and product.

e) Selectivity

The selectivity of catalyst is a measure of the extent to which the catalyst accelerates the reaction to form one or more of the desired products. The selectivity usually varies with pressure, temperature, extent of conversion, reactant composition, and the nature of the catalyst.

f) Sintering

The sintering of the supported metal crystallites is a complicated phenomenon. It may result in an overall loss of the area of the support material, or may cause a loss of dispersion of the metal

crystallite in a supported metal catalyst. The rate of sintering increases rapidly with increasing temperature. It varies with the nature of the metal and chemical, morphology of the support, as well as temperature, pressure and time.

2.6.1 Types of Catalyst

Catalyst can be classified base on its phase and the reaction medium into two types i.e., homogeneous and heterogeneous catalysts. A homogeneous catalyst has the same phase or can be dissolved in the reaction medium. A heterogeneous catalyst involves more than one phase; usually the catalyst is a solid and the reactant and products are in liquid or gaseous phases. Sometimes the reacting mixtures are in both the liquid or gaseous phases.

2.7 Synthesis of Solid Catalysts by Coprecipitation Method [77].

Activity and stability of catalyst are strongly related to material properties such as particle size distribution, morphology and crystallinity. These properties are controlled by the method of synthesis.

For the preparation of heterogeneous catalysts two principal methods exist, viz. the impregnation of performed supports with a solution of precursors of the active metal(s), and so-called coprecipitation where one or more metals are precipitated together with the support or its precursor. The first method is not only use at lab scale, but is also widely applied industrially. For a number of catalysts, and especially at large scale, coprecipitation can be very attractive and indeed a large number of commercial catalysts, for example, for methanol production, hydrogenation, steam reforming, and butane oxidation are produced in this way. This method is often considered to be more difficult and indeed requires an accurate control of conditions and hence the use of more complicated equipment.

A benefit of coprecipitation over impregnation is the high attainable metal loading of up to 60%, sometimes up to 80% or even higher, compared to typically <30% metal loading for impregnation. Another benefit is the relatively high metal dispersion. In contrast, a drawback of the

coprecipitation process is the generation of large quantities of salt solutions and the fact that after precipitation the product has to be separated, which is mostly done by filtration. In addition, the catalyst (precursor) will be in powder form, often with a particle size of 5-30 µm, while for many applications a shaped product like a tablet, extrudate, or fluid-bed particle is required. Coprecipitated powders can be shaped, but if after shaping a calcination has to be applied, for example, to achieve mechanical strength, this has to be performed at almost always milder conditions than those for performed supports that may easily be heated to 700°C or even higher.

The objectives of calcination are to adjust the texture with respect to the surface and pore volume, good mechanical resistance, and to decompose and volatilize the various catalyst formed in preparation such as hydroxides. Types of calcination are dependent the operating condition and the removable wanted such as calcinations in air or other atmospheres.

2.7.1 Basic Principles of Precipitation and Nucleation

Though the preparation of coprecipitated catalysts comprises a number of steps, for example, precipitation, filtration, washing, shaping, drying, calcination, and sometimes activation, precipitation is most important, as during that step the basic properties of the catalyst are established. Indeed, catalyst performance can be significantly influenced by just changing the precipitation conditions.

Precipitation comprises three major steps, that is, liquid mixing, nucleation and crystal growth to form primary particles, and aggregation of the primary particles. The nucleation and crystal growth usually proceed simultaneously; it is possible to treat them separately. It is generally agreed that for the formation of monodisperse crystal separation of the nucleation and growth events is key. Especially for multicomponent systems, nucleation is a complex process. It mostly starts with the formation of clusters, which are capable of spontaneous growth by the subsequent addition of monomers until a critical size is reached. The nucleation step strongly depends on both concentration

and temperature. If the nucleation rate is plotted as a function of supersaturation a curve like that in Figure 2.4 is produced.

For multicomponent systems, it is important to operate at high supersaturation levels so the solubility product of all products is simultaneously exceeded, otherwise a possibly undesired sequential precipitation may occur. Supersaturation can be produced in a variety of ways both by physical and chemical methods: cooling of the reaction mixture, evaporation of solvents, direct reaction of ions, redox reaction, hydrolysis and so on, but reaction of ions in aqueous media, by which the solubility product is exceeded, is most commonly practiced. Water is chosen as solvent not only for economic reasons but mainly because solubility for most metal salts is much higher in water than in organic solvents.

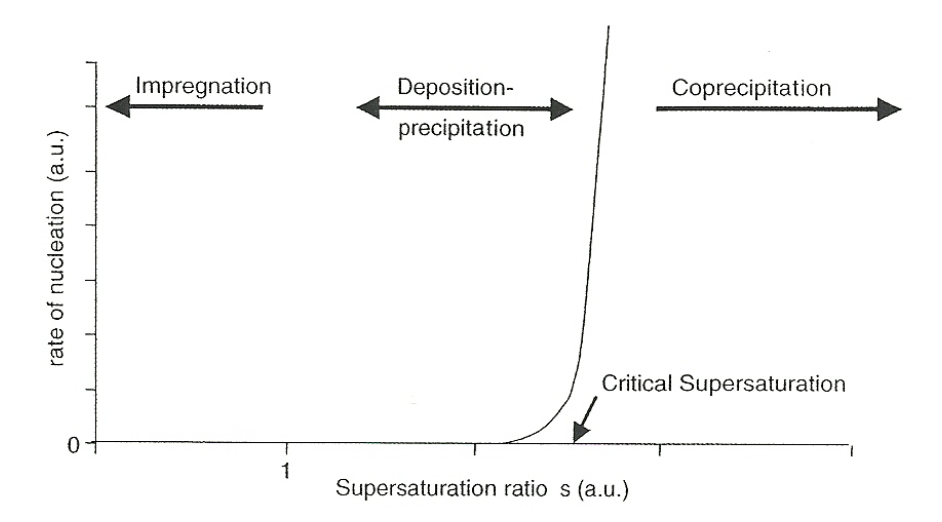


Figure 2.4 The relation between the homogeneous nucleation rate (nuclei per ml/second) and the degree of supersaturation. s = actual concentration/solubility [77].

Apart from nucleation and crystal growth, aggregation is an important process. Aggregation leads to fewer and larger, but yet porous particles. Aggregation is the formation of clusters of nanoscale primary particles into micrometer-scale secondary particles. Physical or chemical forces, such as crystal bridges, can hold these aggregates together. Porosity is then determined by how the primary particles are stacked, and pores can be considered as voids between the primary particles. Other processes, apart from aggregation, which could take place during precipitation are recrystallization (Ostwald ripening) and a change in chemical composition or a change in phase composition.

2.7.2 Precipitation Condition

The primary precipitation products are not necessary the thermodynamically most stable products and usually, depending on the process conditions, counterions like carbonate, sulfate, nitrate, or chloride initially incorporated, are later partially or largely displaced by hydroxide. This displacement process is promoted by high pH and temperature, or by prolonged aging. Thus, when precipitating nickel nitrate with sodium carbonate, for example, at ambient temperature and a pH close to neutral, the kinetics dictate the formation of a nickel precipitate with high levels of nitrate and carbonate incorporation, while the thermodynamics favor a product closer to the hydroxide. Therefore, during aging this product is gradually transformed into a nickel-hydroxide-like product while releasing CO₂ (and nitrate). At higher pH and temperatures this process may, in principle, proceed to a high degree of completion. The final product, however, may still contain some carbonate, and less so nitrate, because eventually in the equilibrium situation, the stability of the products, and the concentration or reactants present, may determine the end product composition.

2.8 Gold Catalysts [78]

As is well known, gold is the most chemically inert metal, and as such the most noble metal. However, when it is represent as particles of nanosize (<5 nm), it becomes reactive. This may be due

to the increasing fraction of low coordination surface sites as particle size decreases, on which, for instance, CO molecules can adsorb, and H_2 can dissociate. This may be due also to changes in the electronic properties exemplified, for instance, by the contraction of the Au-Au bond when the gold particles are smaller than ~ 2 nm.

For years, gold was considered as a poorly active catalyst. In 1987, Haruta and his group discovered that gold particles were exceptionally active in the reaction of CO oxidation at room temperature and even much below, provided that the particles were smaller than 5 nm and supported on a reducible oxide support [13-14]. Since then, gold has been extensively studied, and in many other reactions.

The small size of gold particles is a crucial parameter to obtain active catalysts, not only for CO oxidation but for many other reactions. The methods of preparation that lead to such types of catalysts are therefore very important.

Impregnation to incipient wetness, which is the simplest method, and that can be applied to almost any kind of supports, was the first method used for the preparation of supported gold catalysts with tetrachloroauric acid or gold trichloride as precursor. However, thermal treatments performed to form metallic gold led to large particles (>10 nm) even for low gold loading, and to poorly active catalysts. The formation of large particles is now known to be due to the chlorides, which promote gold particle sintering during thermal treatments.

Haruta *et al.* [13-14]. was the first group to develop other methods of preparation that led to the formation of small gold particles, and as a consequence to active catalysts. The first one was coprecipitation, and the second one was deposition-precipitation.

The gold precursor most used for catalyst preparation is tetrachloroauric acid (HAuCl₄•3H₂O) whose gold is in the oxidation state III. This is a solid, orange in color, hygroscopic, and commercially available. When it is dissolved in water, chloroauric anions hydrolyze and form hydroxo-chloro gold(III)

complexes, $[Au(OH)_xCL_{4-x}]^{-}$. The extent of hydrolysis depends on the pH, the ionic strength, the equilibration time, and the temperature of the solution. These results, mostly based on XAFS and Raman experiments, do not report the presence of neutral gold species, as predicted by thermodynamic calculation.

Care must be taken to avoid uncontrolled reduction of gold during the drying step or sample storage after preparation, especially when gold is supported on titania. To avoid this problem it is advised to dry the samples at room temperature under vacuum and to store them in a refrigerator or a freezer or in a desiccator under vacuum and in the dark. The thermal treatments performed to reduce supported gold precursors into Au⁰ often consist in "calcination" treatments in air because the stability of Au₂O₃ induces the formation of metallic gold. Finally, the question of hazards of explosive "fulminating" gold, which is a family of ill-defined gold compounds containing nitrogen, must be addressed. Reports mention that supported gold catalysts must never be prepared with solutions containing both gold salts and ammonia because the gold-nitrogen compounds contained in dried catalysts are extremely shock sensitive, and may explode. Other authors using ammonia, cyanide, or urea during catalyst preparation did not report such a problem. In any case, this type of catalysts must certainly be handled with care since the chemistry of "fulminating" gold is not well known.

2.8.1 Preparation Involving Aqueous Solutions

a) Impregnation to Incipient Wetness

In order to attempt to solve the problem of gold sintering because of the presence of chloride, impregnation with gold salts free of chlorides was performed. Gold acetate (Au^{III}(O₂CCH₃)₃) or potassium aurocyanide (KAu^I(CN)₂) led to smaller particles (~5 nm) than HAuCl₄. However, gold acetate is hardly soluble in water, and when KAu(CN)₂ is used, potassium, which is deposited onto the support, may have an influence on the catalytic properties.

b) Deposition-Precipitation with NaOH

This method of deposition-precipitation is probably the most used for the preparation of gold catalysts since it readily leads to the formation of small gold particles (2-3 nm). This method was first proposed by Haruta *et al.* [13-14]. The pH of the solution containing HAuCl₄ and the oxide support is adjusted by addition of NaOH, often 7-8 for titania or alumina. The suspension is stirred for ~ 1 hour at 70-80°C. The catalyst is then washed with water to eliminate as much chloride and sodium ions as possible, dried between room temperature and 100°C, then usually calcined in air.

This method of deposition-precipitation is suitable for oxide supports whose point of zero charge (PZC) is higher than 5, such as MgO, TiO₂, Al₂O₃, ZrO₂, CeO₂. It is not suitable for SiO₂ (PZC ~2), SiO₂-Al₂O₃ (PZC ~1), WO₃ (PZC ~1) or for supports such as activated carbon or zeolites due to their high acidity.

2.8.2 Special Methods

Sonochemical Techniques

Gold particles can also be simultaneously deposited and reduced on a support by sonication. Sonication induces chemical changes due to cavitation phenomena involving the formation, growth, and implosive collapse of bubbles in liquid, which lead to the decomposition of water molecules in H and OH radicals. The H radicals can trigger, for instance, the reduction of Au^{III} species in solution.

This method has been developed by Gedanken's group. It was applied for the deposition of gold on silica submicrospheres, and on powders of silica and titania after immersion in a solution of $HAuCl_4$ in water or ethylene glycol basified with ammonia. The suspension was sonicated under Ar or Ar and H_2 (5%). After sonication, washing, drying, and also calcinations in the case of silica submicrospheres, gold particles of ~4-5 nm on average were obtained, and all gold was deposited onto the supports (7 or 5 wt%). Sonication was also used to avoid aggregation of gold colloids and to favor the interaction with the support.

2.9. Oxidative coupling of methane

Since the pioneering work of Keller and Bhasin in 1982 [79], much more attention has been paid to the production of C2 hydrocarbons from oxidative coupling of methane. Effective catalysts are important for OCM, many studies have been focused on the design and development of catalysts for OCM [80,58, 81]. In the OCM process (at about 800 °C), the following selective and nonselective reactions occur simultaneously [82].

$$2CH_4 + 1/2O_2 \longrightarrow C_2H_6 + H_2O + 174.2 \text{ kJ/mol}$$
 (13)

$$C_2H_6 + 1/2O_2 \longrightarrow C_2H_4 + H_2O + 103.9 \text{ kJ/mol}$$
 (14)

$$C_2H_6 \longrightarrow C_2H_4 + H_2 - 103.9 \text{ kJ/mol}$$
 (14)

$$CH_4 + 2O_2 \longrightarrow C_2H_4 + H_2O + 103.9 \text{ kJ/mol}$$
 (16)

$$CH_4 + 1.5O_2 \longrightarrow CO + 2H2O + 519.1 \text{ kJ/mol}$$
 (17)

According to the accepted mechanism, the oxidative methane activation in the catalytic OCM process involves an abstraction of H-atom from methane, leading to the formation of methyl radicals on the catalyst surface; the two desorbed methyl radicals are coupled in the gas phase to form ethane molecule [82, 83]. Since the pioneering work of Keller and Bhasin [79] (which was based on the use of reducible metal oxide catalysts), the oxidative coupling of methane (OCM) to C2 hydrocarbon has been widely investigated. A large number of catalysts, mostly bi-or multicomponent mixed or supported metal oxides containing components with basic properties such as oxides of alkali metals, alkaline earth metals, rare earth metals have been studied. The basicity surface of catalysts as a precondition of catalytic effectiveness was often noticed with heterolytic C–H bond splitting in methane. However, the activity and selectivity of the catalysts showed dependence on both the surface acidity and basicity but the relationship between the acidity/basicity properties and catalytic

performance was shown to be rather complex. There are also known examples when the decrease in basicity becomes beneficial and prevents the formation of poisoning carbonate from CO₂ produced in OCM. Stronger acid sites were found to be harmful for the C2 selectivity.

The major problems of OCM reaction are the low C2 products yield and hot spot temperature. The C2 products yield in a conventional fixed bed reactor was limited to about 25%]. This is due to the presence of undesired complete oxidation reactions in the gas phase and partially on the catalyst surface. As found from the OCM kinetics [84], the deep oxidation of methane to CO and CO₂ are the main problem. A lower oxygen partial pressure is favorable in achieving in higher C2 selectivity. Therefore, distributing the oxygen along the reactor length is an important strategy to improve the performance. A membrane reactor was proposed to control the distribution of oxygen to the catalyst bed due to methane does not directly contact with oxygen, methane combustion reaction can be avoided from the explosion problem. Moreover, the heat of reaction released to the catalyst bed can be much more flat throughout the reactor cross-section; thereby the hot spot temperature is less severe.

2.9.1 Perovskite-based Catalyst for Oxidative Coupling of Methane

Peña and Fierro [76] explained about the perovskite materials for oxidative coupling of methane as following detail. Elshof *et al.* [85] studied the oxidative coupling of methane on a $La_{0.6}Sr_{0.4}Co_{0.8}Fe_{0.2}O_3$ membrane using O_2 partial pressures between 0.01 and 1 bar. Methane was converted to C_2H_6 and C_2H_4 with selectivities of up to 70% but at conversion levels of only about 1-3%. An important requirement for the reaction is that the O_2 flux should be limited by exchange kinetics, because otherwise reduction of the membrane would occur, with the subsequent decrease in C_2 selectivity. The same reaction was studied in a membrane reactor with $BaCe_{0.8}Gd_{0.2}O_{3.\delta}$, which is a mixed oxide ion-electron hole conductor. By passing CH_4 over one side of the membrane and O_2 over the other side, reasonable conversions of methane were obtained, with much greater selectivity

than when both CH_4 and O_2 were fed to the same side of the membrane. This means that the O species released from the membrane at the CH_4 side is more active for C_2 formation than gaseous O_2 . In addition, the use of highly permeable ceramic membranes with a catalytically active surface for the coupling reaction affords one the possibility of achieving much higher C_2 yields than with a packed-bed reactor. The high C_2 yield can only be attained when the oxygen flux, the CH_4 flow rate, and the intrinsic reaction rate match each other.

Other perovskite membranes display proton conductivity when exposed to a H-containing atmosphere at high temperatures. Au/LaSrMnO₃ and LaSrCrO₃ perovskite composite catalysts have been investigated as potential anode catalysts in SOFCs for propane reforming processes [8]. Au/LaSrMnO₃ showed a higher activity for propane reforming than Au/LaSrCrO₃. Iwahara et al. [86-87] discussed the application to steam electrolysis to produce H₂ gas on proton conductive MCeO₃ (M = Sr, Ba) perovskites. Hamakawa et al. [88] reported data on CH_4 coupling using $SrCe_{0.95}Yb_{0.05}O_{3-\delta}$ (SCYO) as a solid electrolyte in an electrochemical cell. Because there is no gaseous O2, which is responsible for the combustion reaction, this may lead to a much better C2-selectivity than can be obtained with the conventional catalytic process. Chiang et al. [89] also investigated the dehydrogenative dimerization of methane using SCYO proton-conducting membranes and proposed that the rate-determining step is the formation of a CH₃·radical by proton abstraction. Comparison of the activity data using different reactors for this reaction indicates that the SCYO membrane reactor affords a substantially larger yield than the corresponding conventional catalytic reactor. The experimental results clearly show that the equilibrium conversion of the dehydrogenation reaction can be dramatically changed by using a proton-conducting membrane in an electrochemical reactor cell.

Later investigator investigated OCM to C₂ hydrocarbon over Mn/Na₂WO₄/SiO₂, Mn/K₂WO₄/SiO₂ catalyst, and this showed the best C₂ selectivity but provided the C₂ yield of only 4%-7% (Zheng *et al.*, [90]), (Chen *et al.*, [91], (Wang *et al.*, [92], (Bhatia *et al.*, [86]). Moreover the performance of Mn-

Na₂WO₄/SiO₂ catalyst to promote Ce that increased its activity and stability ((Li *et al.*, [94], (Shahri and Pour, [95]). Although theses catalysts were reported to be a good catalyst for the OCM in fixed bed reactor because Na₂WO₄, and Mn₂O₃ species are the active sites of the catalyst. They are very important in achieving high selectivity of C2 hydrocarbon products. However one of problem to apply Mn/K₂WO₄/SiO₂ and Mn/Na₂WO₄/SiO₂ into anode catalyst for SOFC is SiO₂ support and Mn/Na₂WO₄, which has a low the electrical conductivity that effect to power density. Moreover thermal expansion coefficient of SiO₂ mismatch with YSZ electrolyte. Although changed SiO₂ to other support such as YSZ support, power density is still low. The main reason is really that Na₂WO₄Mn₂O₃ has low the electrical conductivity because of phases structure of Na₂WO₄. Therefore investigation new catalysts should indeed be concerned.

CHAPTER 3

METHODOLOGY

The experimental procedures for $La_{0.6}Sr_{0.4}MnO_3$ (x ≈ 0.4), Na_2WO_4 -Mn preparation and gold deposition are explained in this chapter. The properties of these prepared samples were characterized by various techniques. Then, the catalytic performance of the catalyst toward oxidative coupling of methane was examined. The SOFC reactor are designed and fabricated for oxidative coupling of methane. The Details of this chapter are described in three main parts; catalyst preparation, characterization of synthesized catalyst, and catalytic performance evaluation.

3.1 Catalyst Preparation

The preparation methods of catalyst are composed of three sections i.e., $La_{0.6}Sr_{0.4}MnO_3$ perovskite preparation, gold deposition on perovskite and 5 wt%Na₂WO₄–2 wt%Mn/SiO₂.

3.1.1 Preparation of La_{0.6}Sr_{0.4}MnO₃ Perovskite Material

 $La_{0.6}Sr_{0.4}MnO_3 \ (x \approx 0.4) \ perovskite \ was \ prepared \ by \ coprecipitation \ technique. \ La(NO_3)_3,$ $Sr(NO_3)_2, \ and \ Mn(NO_3)_2\cdot 4H_2O \ were \ used \ as \ starting \ materials \ (Figure \ 3.1) \ . \ Initially, \ stoichiometric$

amounts of metal nitrates were dissolved in deionized water. Hence, an aqueous solution of citric acid and ethylene glycol was added to the metal solution (citric acid:metal nitrates[acetate]: ethylene glycol molar ratios=5:1:4.3). The mixture was stirred at 70 °C for 12 h. Water was then slowly evaporated on a hot plate and the resulting brown gel was dried and then heated up in air at 400 °C for 2 h in an oven. La1 $_{-x}$ Sr $_x$ MnO $_3$ (x \approx 0.4) perovskite samples (hereafter LSM) were obtained by ball-milling the decomposed resin for a few hours before calcination at 1000 °C for 2 h in air (heating rate 20°C/min). The calcination process was applied in order to eliminate water and other remaining substances so it could be important effect of physical properties of catalyst.

3.1.2 Gold Deposition

After preparing La_{0.6}Sr_{0.4}MnO₃ perovskite, gold particles were deposited on the prepared samples (Figure 3.2). The selected technique for gold deposition on perovskite materials is deposition-precipitation technique integrated with ultrasound-driven. The advantages of this technique are the ability to form metallic nanoparticles with uniform shape, narrow size distribution and high purity. First step, gold precursor solution was prepared by dissolving the desired weight amount (1wt.%Au) of HAuCl₄ (Tetrachloroauric (III) acid) in deionized water, followed by the addition of an ammonia solution until a final pH of 7 was reached. Then, Au precursor was added to stirred LSM, which was then sonicated in an ultrasonic bath for 6 h; next, it was centrifuged, washed with deionised water, dried and heated at 300°C for 4 h in air.

3.1.3 Preparation of 5 wt%Na,WO₄-2 wt%Mn/SiO,

 $5 \text{ wt}\% \text{Na}_2 \text{WO}_4 - 2 \text{ wt}\% \text{Mn/SiO}_2 \text{ catalyst (denoted by Na-W-Mn/SiO}_2)}$ was prepared by a two-step incipient wetness impregnation method. In the first stage, manganese was impregnated onto SiO_2 support (60-100 mesh size silica gel, Davisil grade 645 from Aldrich) with an 5 wt% concentration of $\text{Mn(NO}_2)_3.6\text{H}_2\text{O}$ (Aldrich) solution. Then the sample was dried at 110°C overnight. In

the second stage, 2% wt of Na₂WO₄.2H₂O (Aldrich) solution was added to the support sample. The impregnated silica particles were dried again and calcined in air at 850°C for 5 h. For comparison, the 5 wt%Na₂WO₄–2 wt%Mn/YSZ and 5 wt% Na₂WO₄-2 wt%Mn/LaAlO₃ catalysts (denoted by Na-W–Mn/YSZ and Na-W-Mn/LaAlO₃, respectively) were prepared by the same method. Herein, YSZ particles (8 mol% Yttria-Stabilized Zirconia, TZ-8Y, Tosoh, Japan) were selected as a support, while LaAlO₃ was synthesized by following the procedure described elsewhere [13].

3.2 Characterization of Synthesized Catalyst

The synthesized catalysts were determined their properties by various techniques; BET, XRD, XRF, SEM, and TEM.

- Brunauer-Emmett-Teller (BET): The specific surface area and pore size of catalysts was measured by using the BET surface area analyser ASAP 2000. This method used nitrogen (N₂) adsorption isotherm. Adsorption always occurs when a solid surface is exposed to vapor
- X-Ray Diffractometer (XRD): The crystalline phases of prepared samples were identified by x-ray diffraction technique using Cu-K α radiation. The x-ray diffractograms were recorded in range of 20 $^{\circ}$ to 80 $^{\circ}$ (2 θ).
- Scanning Electron Microscopy (SEM, JEM-6400 Jeol Ltd., Japan): The surface morphology and particle size of prepared samples were investigated by using scanning electron microscope at magnification of 15,000x.
- Transmission Electron Microscopy (TEM): The gold particle size of Au/perovskite catalysts were determined by picture from transmission electron microscopy (JEM-2100, Jeol Ltd., Japan). Specimens were prepared for TEM analyses by depositing a drop of a suspension obtained by ultrasonic dispersion of the catalysts in ethanol onto a carbon-supported film.

• XPS analysis of catalysts was performed to determine composition in the near-surface of catalysts. An Mg target was used as the anode of the X-ray source with a power of 200 W. The constant pass energy of the analyzer is 30 eV. The binding energies were calibrated using the C(1s) line at 285.0 eV as the reference.

3.3 Catalytic Activity Test

The catalytic reactions of methane were tested by two systems, by conventional type reactor (fixed bed reactor) and solid oxide fuel cell type reactor. Conventional reactor; The catalytic reactions of methane over LSM , Au/LSM , 5 wt%Na₂WO₄–2 wt%Mn/SiO₂ ,5 wt%Na₂WO₄–2 wt%Mn/YSZ and 5 wt% Na₂WO₄–2 wt%Mn/LaAlO₃were performed at atmospheric pressure and at temperatures of 1073-1273 K in a quartz microreactor (i.d. 6 mm) placed in a ceramic tube furnace. A fresh catalyst was loaded into a reactor that was located in a programmable furnace with a thermocouple placed in the centre of the catalyst bed, 2:1 and 6:1 CH₄:O₂ molar ratios of the feed were used without using any diluents.

3.3.1 Experimental Set Up for Oxidative Coupling of Methane in Fixed bed reactor

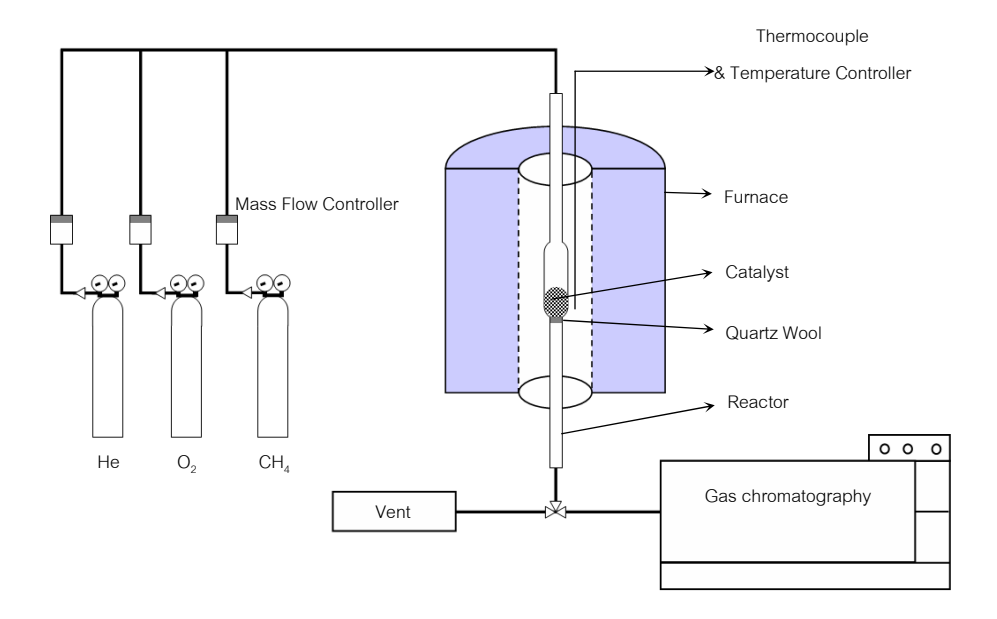


Figure 3.1: Schematic diagram of oxidative coupling of methane system

Schematic diagram for the experimental system of oxidative coupling of methane is shown in Figure 3.3. This system was constructed with three main sections i.e., supplied gases, reaction zone, and analysis section.

The supplied gases composed of 99.999% helium, 5% methane, and air. They were used without further purification. The ratio of mixing gases were dependent the purpose of each experiment. For each gas cylinder, the pressure regulator was installed at the outlet in order to set the constant pressure to the mass flow controller. The mass flow controllers were installed for adjusting the flow rate of inlet gases.

The reaction in fixed bed reactor was carried out in a tubular quartz reactor filled with 0.3 g of selected sample and small amount of quartz wool. The reactor was vertically mounted inside a furnace. Gas mixture between methane and air were continually flown into the reaction zone at total flow rate 200 cm³·min⁻¹. The reactions were studied in temperature range of 800-900°C (heating rate of 10°C·min⁻¹) and held around 3 hours until equilibrium was reached. For other parameters, they

were described in experimental procedures. After reaction, the composition of effluent gas was analyzed by online gas chromatography and TCD detector (shimadzu company).

The schematic diagram of the solid oxide fuel cell reactor was shown in Figure 3.2 It was separated with two ceramic tubes (O.D. = 25 mm), between which the cell system was placed and sealed with ceramic seal (Aremco 885, Aremco Products, Inc., Valley Cottage, NY). The effective area of the anode was 1.9 cm³. Platinum wires of 0.5 mm diameter (Alfa Aesar) were connected to platinum meshes (100 mesh, Alfa Aesar) placed on both electrodes to serve as current collectors. 6.7×10⁻⁷ mol.s⁻¹ of methane was fed to the anode without mixing gas, and 3.3×10⁻⁵ mol.s⁻¹ of air was fed to the cathode in the temperature range of 1073-1273 K. Product analysis during operation were detected using an on-line gas GC-8A gas chromatograph (Shimadzu) equipped with a TCD, using a Poropak Q and 5A Molecular Sieve column every 30 min. Current and voltage values were measured using a current meter at the closed circuit condition and using a voltmeter at the open circuit condition, respectively.

The terms of the reaction performance were defined as follows:

Conversion of methane
$$(X_{CH_4}, \%) = 100 \times \frac{V_0[CH_4]_0 - V[CH_4]}{V_0[CH_4]_0};$$

Selectivity of C2
$$(S_{c_2},\%) = 100 \times \frac{(V[C_2H_6]_0 + V[C_2H_4]_0) \times 2}{V_0[CH_4]_0 - V[CH_4]};$$

Selectivity of CO
$$(S_{CO},\%) = 100 \times \frac{V[CO]}{V_0[CH_4]_0 - V[CH_4]};$$

Selectivity of
$$CO_2(S_{CO_2},\%) = 100 \times \frac{V[CO_2]}{V_0[CH_4]_0 - V[CH_4]};$$

Yield of C2 (%) =
$$\frac{X_{CH_4}S_{C_2}}{100}$$
.

3.3.2 Preparation of electrode

A plate -type YSZ (8 mol% Y_2O_3 , thickness = 0.3 m, diameter = 25 mm, FCM) was used as an electrolyte. Normally, perovskite type $La_{0.85}Sr_{0.15}MnO_3$ (LSM) was used as a cathode materials. LSM powders were described somewhere else [8]. LSM perovskite samples were decomposed to fine powders. The LSM powder was mixed with glycerol and pasted on the outside of YSZ plate. It was heated at 1273 K for about 2 h in air. The anode catalyst was prepared on the other side of YSZ plate by paste method, the same method as for the LSM cathode. 1%Au/LSM was used as anode catalysts. In additional 5 wt%Na₂WO₄-2 wt%Mn/YSZ was also used as anode.

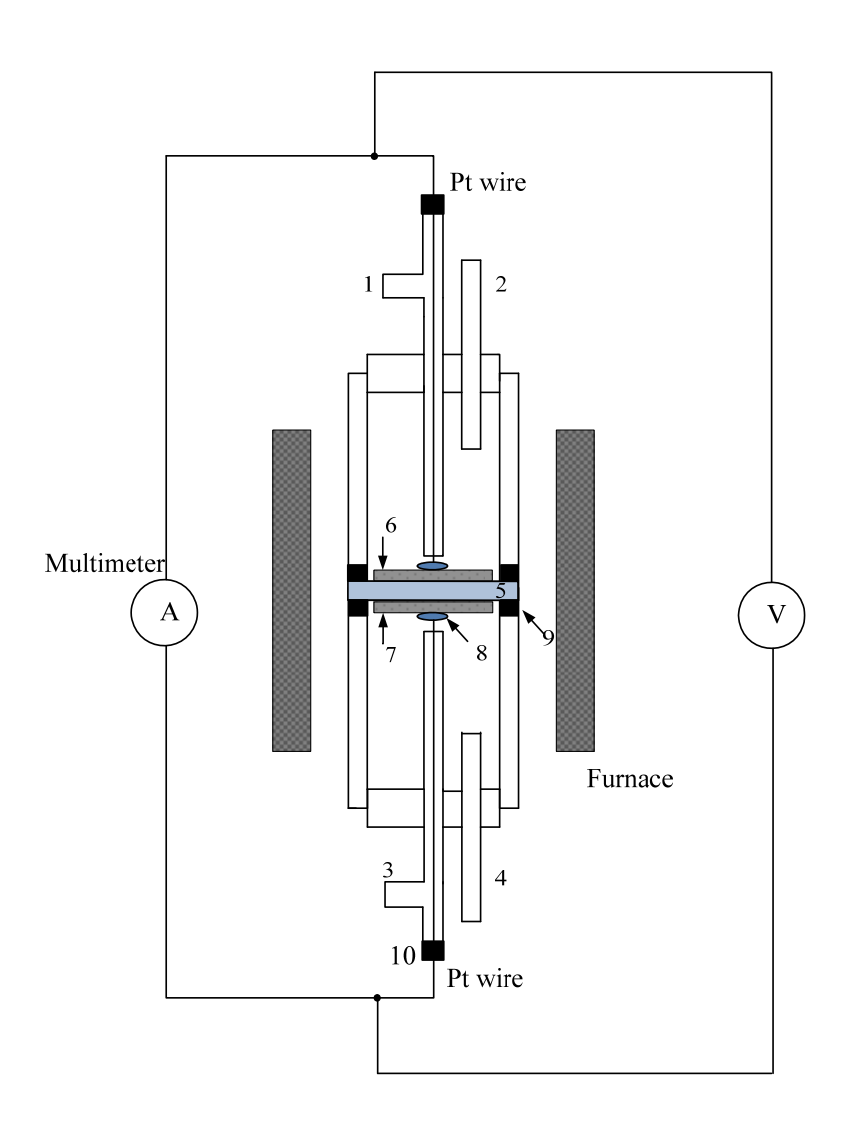


Figure 3.2 Schematic diagram of oxidative coupling of methane system in SOFC reactor

1. Anode side feed (CH₄)

2. Exit gas from anode side

3. Cathode side feed (Air)

4. Exit gas from cathode side

5. YSZ plate

6. Cathode electrode (La_{0.85}Sr_{0.15}MnO₃)

7. Anode electrode (Au/LSM)

8. Pt mesh

9. Pyrex ring

10. Silicon plug

3.3.3 Experimental Procedures

The aim of this research is to study the potential of catalyst for OCM reaction. At this stage, the prepared materials consisted of $La_{1-x}S_xMnO_3$ ($x\approx 0.4$) c, Au supported on $La_{1-x}S_xMnO_3$ ($x\approx 0.4$). 5 wt%Na₂WO₄-2 wt%Mn/SiO₂ ,5 wt%Na₂WO₄-2 wt%Mn/YSZ and 5 wt% Na₂WO₄-2 wt%Mn/LaAlO. These materials were evaluated the catalytic activity toward OCM in fixed bed reactor and SOFC reactor

The operating parameters that effect to light hydrocarbon production via OCM reaction, for example, CH₄:O₂ ratio, operating temperature, atmospheric condition during heating up process.

These parameters were studied and optimized for good catalytic performance.

CHAPTER 4

RESULTS AND DISCUSSION

The results and discussion shows 2 part ; first, The evaluation of Au/LSM, and second : 5 wt%Na $_2$ WO $_4$ -2 wt%Mn/SiO $_2$,5 wt%Na $_2$ WO $_4$ -2 wt%Mn/YSZ and 5 wt% Na $_2$ WO $_4$ -2 wt%Mn/LaAlO . These catalysts performance toward the oxidative coupling of methane are composed of three main tasks i.e. La $_{1-x}$ S $_x$ MnO $_3$ (x \approx 0.4) perovskite 5 wt%Na $_2$ WO $_4$ -2 wt%Mn/SiO $_2$,5 wt%Na $_2$ WO $_4$ -2 wt%Mn/YSZ and 5 wt% Na $_2$ WO $_4$ -2 wt%Mn/LaAlO preparation, and catalytic activity testing. The effects of various OCM conditions are also carried out. The results of each part are described as following:

Part I :Au/LSM

4.1 Characteristic of Synthesized Au/LSM Catalysts

The BET surface area of our LSM was 6.84 m²/g, the pore volume was 0.009 cm³/g, and the pore size was 7.2 nm as summarized in Table 1. These results are in good agreement with several

reports. After LSM loading with 1%, 3%, 5 wt% Au precursor, the surface areas and pore sizes of the LSM and Au/LSM decreased because of the drying and calcination processes.

The XRD pattern of LSM was identified to be perovskite type crystalline structure (Fig. 1a). The crystallite size of $La_{0.6}Sr_{0.4}MnO_3$ estimated by the well-known Scherrer equation was around 60-100 nm. The XRD pattern of Au/LSM nanocomposites (Figs. 1b, c, and d) revealed the additional peaks at $2 = 38.41^{\circ}$ and 64.95° . As shown in Fig. 1c, the Au size of 3% wt Au/LSM estimated by Scherrer equation was around 15-20 nm. After the reaction, as shown in Figure 1e, the size of spent Au catalyst was estimated around 30-40 nm.

Fig. 2 shows TEM images of LSM and the 1%, 3%, 5wt%Au/LSM nanocomposites. The TEM micrographs of LSM show the presence of compact nanocrystalline agglomerates. The estimated particle diameters for LSM and Au were 100-400 nm and 10-30 nm, respectively. The Au morphology was mostly found in hemispherical shape. A less homogenous dispersion of metallic Au nanoparticles having dimensions from < 5 nm up to 20-25 nm on LSM surface was obtained when 3 and 5 wt.% of Au were added to the LSM suspension.

Table 1 Surface areas, average pore size and pore volume

Catalyst	surface area (m² g⁻¹)	Total pore volume (cm ³ g ⁻¹)	Mean pore diameter (nm)
LSM	6.84	0.009	7.2
1%Au/LSM	5.34	0.007	5.9
3%Au/LSM	4.47	0.007	5.2
5%Au/LSM	3.40	0.004	4.1

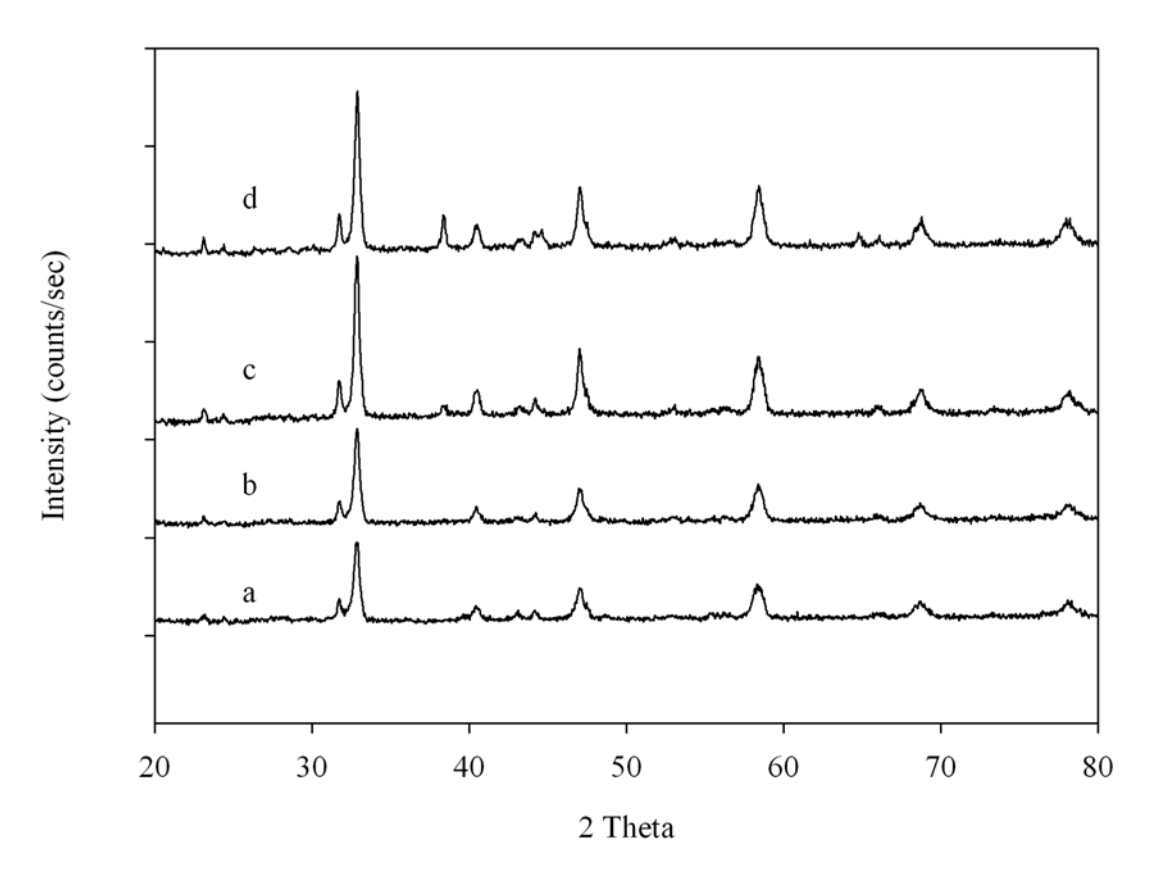


Fig. 2. XRD patterns of (a) LSM, (b) 1%wt Au/LSM, (c) 3%wt Au/LSM, (d) 5%wt Au/LSM

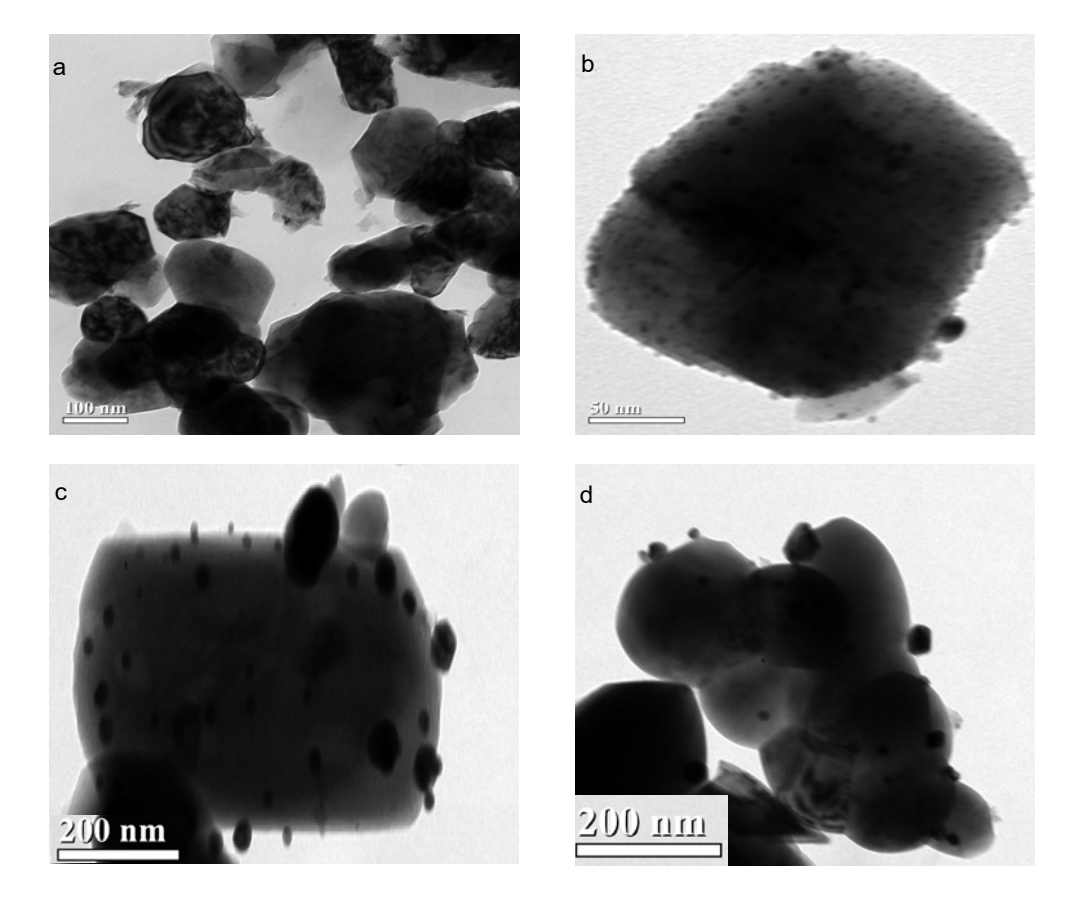


Fig. 3. TEM images of (a) LSM and (b,c,d) 1%wt Au/LSM and 3%wt Au/LSM

4.2 Catalytic performance of catalysts in fixed bed reactor

As for the conversion of methane, typically, OCM has been studied mostly in conventional reactors such as fixed bed reactor. One of attractiveness for selecting methane is its utility for various applications, its wide availability. Table 2 summarises the catalytic performances of LSM and Au/ LSM at 7860 h^{-1} of GHSV and at 1073 K for a molar ratio of CH_4/O_2 = 6:1. For Au/LSM, the presence of Au can improve the catalytic performance of LSM. The conversion of CH₄ was slightly increased, from 10.6 to 12.9%, (1 wt%, 3 wt% and 5 wt% Au). The selectivity of C2 was slightly improved with the increasing Au concentration, from 16.0% at 1 wt%, to 17.8% at 3 wt%. However, C2 selectivity of the 5 wt% Au addition to LSM powders was obviously decreased when compared with the 1 wt%, 3 wt% Au because Au nano-particles have agglomerated and the catalytic performance is significantly affected by the size of the Au particle. These results are in agreement with the data obtained from TEM micrographs at 5 wt% Au/LSM. In addition, the trend of C2 yield was imperceptible from 1.0 % to 1.9 % at GHSV of 7860 h⁻¹ and 1073 K., which is similar to the CH₄ conversion. A comparison between LSM and Au/LSM catalysts obviously indicates that when Au/LSM is utilised in the OCM reaction, the % conversion, % selectivity of C_2 hydrocarbons and % $\mathrm{C}2$ yield are greater than those of LSM. Therefore, the Au nanoparticle can be concluded to promote the catalytic performance in which

these results support the previous finding. As a result from this work, Au/LSM is a potential anode catalyst for further application in SOFC-type reactor for the cogeneration of chemicals and electricity.

Table 2 Catalytic performance of LSM and Au/LSM at different Au loading (CH₄:O₂=6:1, 1027 K and GHSV= 7860 h⁻¹)

Catalyst	Conversion	Selectiv	Selectivity (%)			
	(%)				(%)	
	CH ₄	C_2	СО	CO ₂	C2	
LSM	6.8	14.8	20.2	64.4	1.0	
1%Au/LSM	10.6	16.0	24.3	53.0	1.7	
3%Au/LSM	10.8	17.9	17.2	59.6	1.9	
5%Au/LSM	12.9	11.3	23.8	53.5	1.5	

4.3 Catalytic performance of catalysts in SOFC reactor

An LaSrMnO₃ cathode //YSZ// Au/LSM Anode cell was tested under a concentration cell operation. Argon was fed into the anode (3% Au/LSM) and air was fed into the cathode (LaSrMnO₃). The electro motive force (e.m.f.) and closed circuit current are shown in Table 3. When methane was not present in the anode side in this operation, the e.m.f. is generated by the difference in the partial pressures of oxygen between the cathode and the anode sides. Table 4 shows the activity of anode catalyst for OCM, when methane is fed to the anode side in Air/ LaSrMnO₃ cathode //YSZ// Au/LSM

anode catalyst, the e.m.f. and closed circuit current increased to 0.865 V and 9.8 mA, respectively at 1123 K. The e.m.f. was also close to the theoretical value of oxidation of methane. It should be noted that the oxygen leakage from the surrounding to the cell should be small since the oxygen flux calculated from the current is in good agreement with the rate of oxygen present in the products at the anode side. From the experiments at 1123 K, the methane conversion was around 4.4% and 11.6% for C2 hydrocarbons selectivity observed with a significant CO production. The methane conversion increases with increasing operating temperature due to the oxygen flux arise with increasing temperature. However, the C2 selectivity was very low as the Au/LSM seems to be active for partial oxidation, not the OCM reaction. These results demonstrated that the cogeneration of C2 hydrocarbon especially ethylene which is a basis for chemical industry was possible in an SOFC reactor. To achieve this task, it requires further improvement for anode electrode in the SOFC reactor system. In addition, it should be noted that the stability of the SOFC reactor is also a very important issue in real operation.

Table 3 Fuel cell of e,m.f. and current

Temperature (K)	e.m.f.	Current
	(V)	(mA)
1023	0.13	0.8
1073	0.19	1.0
1123	0.23	2.4

Cathode: Air = 30 ml/min , Anode: Argon= 30 ml/min

4.4 Conclusions

A possibility in simultaneous generation of electrical energy and C2 hydrocarbons over Au/LSM in an SOFC reactor can be drawn from the combined investigations in this research. The

characterization results showed that Au nanoparticles could significantly improve the catalytic performance of the composite. The effect of Au addition of 1 wt% and 3 wt% to LSM showed some influences on C2 selectivity, CH₄ conversion, except for 5 wt% which showed no catalytic activity. Thus, it is recommended that Au/LSM is not suitable to use in a methane oxidative coupling process but it is possible to be used in a partial oxidation fixed bed reactor and an SOFC reactor.

Part II Na-W-Mn/SiO₂

4.5 Catalyst characterisation

The BET surface areas, volume and pore size of all catalysts prepared in this work are summarized in Table 4. After the active phase was loaded with Na₂WO₄ and Mn precursor, the surface areas, volume and pore sizes of the SiO₂, YSZ and LaAlO₃ decreased due to a packing effect during the drying and calcination processes. For Na-W-Mn/SiO₂ catalyst, calcinations of the amorphous silica in the presence of an alkali salt like sodium tungstate as a mineralizing agent caused the complete conversion of the silica to the low surface area crystalline phase.

Table 4 Surface area, average pore size and pore volume

Catalysts	surface area	Total pore	Mean pore
		volume	diameter
	$(m^2 g^{-1})$	(cm ³ g ⁻¹)	(nm)
SiO ₂	255.0	0.8778	10.5
YSZ	14.2	0.0964	26.4
LaAlO ₃	4.3	0.0193	17.4
Na-W-Mn/SiO ₂	3.5	0.0043	6.5
Na-W-Mn/YSZ	7.9	0.0405	18.5
Na-W-Mn/LaAlO ₃	4.2	0.0107	7.4

The SEM images in Fig.4 clearly show a congregation of many particles. The Mn distribution determined by EDX spectroscopy (shown in Fig.4 (c-h)) also qualitatively confirms that Mn elements were well dispersed on the SiO₂, YSZ and LaAlO₃ supports. Malekzadeh et al. [96] have reported that manganese oxide (MnO_x) promoted catalyst can decrease band gap of the catalyst. The conductivity of the catalyst depends on the band gap of the metal oxide constituent of the catalyst. MnO_x shows the high electrical conductivity, which could improve a performance in OCM reaction.

X-ray powder diffraction (XRD) was used to identify bulk phase composition in the catalysts. The XRD patterns of YSZ, LaAlO₃, Na-W-Mn/SiO₂, Na-W-Mn/YSZ and Na-W-Mn/LaAlO₃ are displayed in Figs. 5 (a-e). For Na-W-Mn/SiO₂ catalyst, the main phase is Na₂WO₄, Mn₂O₃ and α-cristobalite. For the XRD spectra of Na-W-Mn/YSZ and Na-W-Mn/LaAlO₃, the formation of the Na₂WO₄ and Mn₂O₃ phase were not detected. However, Na₂WO₄ and Mn₂O₃ phases on YSZ and LaAlO₃ support were confirmed by using an X-ray photoelectron spectroscopy (XPS).

Table 5 shows the observed elemental concentrations near to the surface of the fresh catalysts by XPS characterization. These catalysts show that the surface atomic concentrations of Na, W and Mn are close to those of the bulk compositions, indicating that Na, W and Mn are enriched on the catalysts surface. Moreover, two kinds of surface oxygen on the catalysts (the oxygen connected with SiO₂, ZrO₂ or metal atoms) were found. For YSZ and LaAlO₃ supports, Na(1s), W(4f) and Mn(2p) are present clearly on the catalyst surface. This confirms that YSZ and LaAlO₃ supports have the Na₂WO₄ and Mn₂O₃ active species on the catalyst surface.

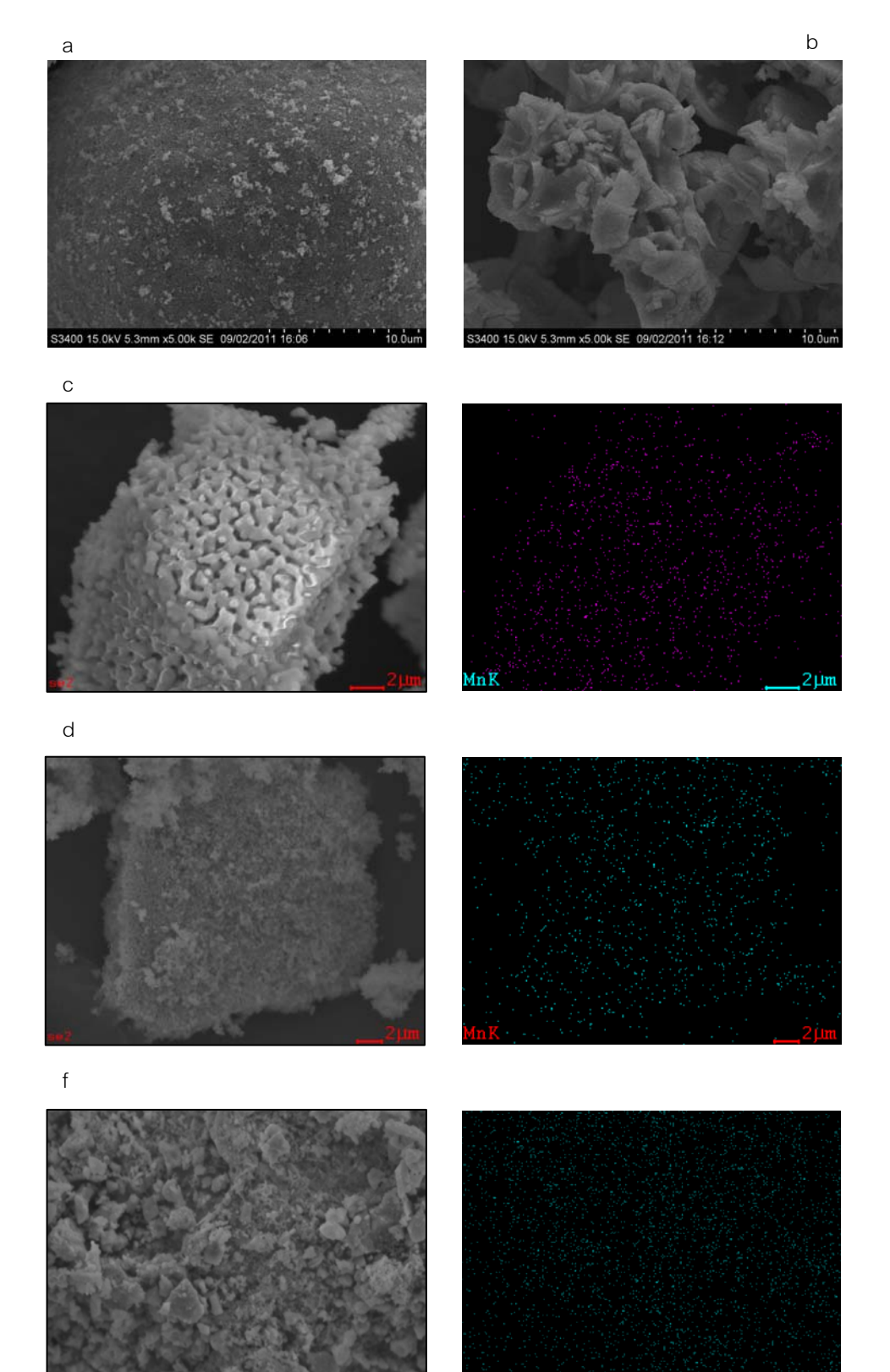


Fig. 4. SEM images and Mn elemental mappings of (a) YSZ, (b) LaAlO $_3$, (c) Na-W-Mn/SiO $_2$, (d) Na-W-Mn/YSZ and (d) Na-W-Mn/LaAlO $_3$

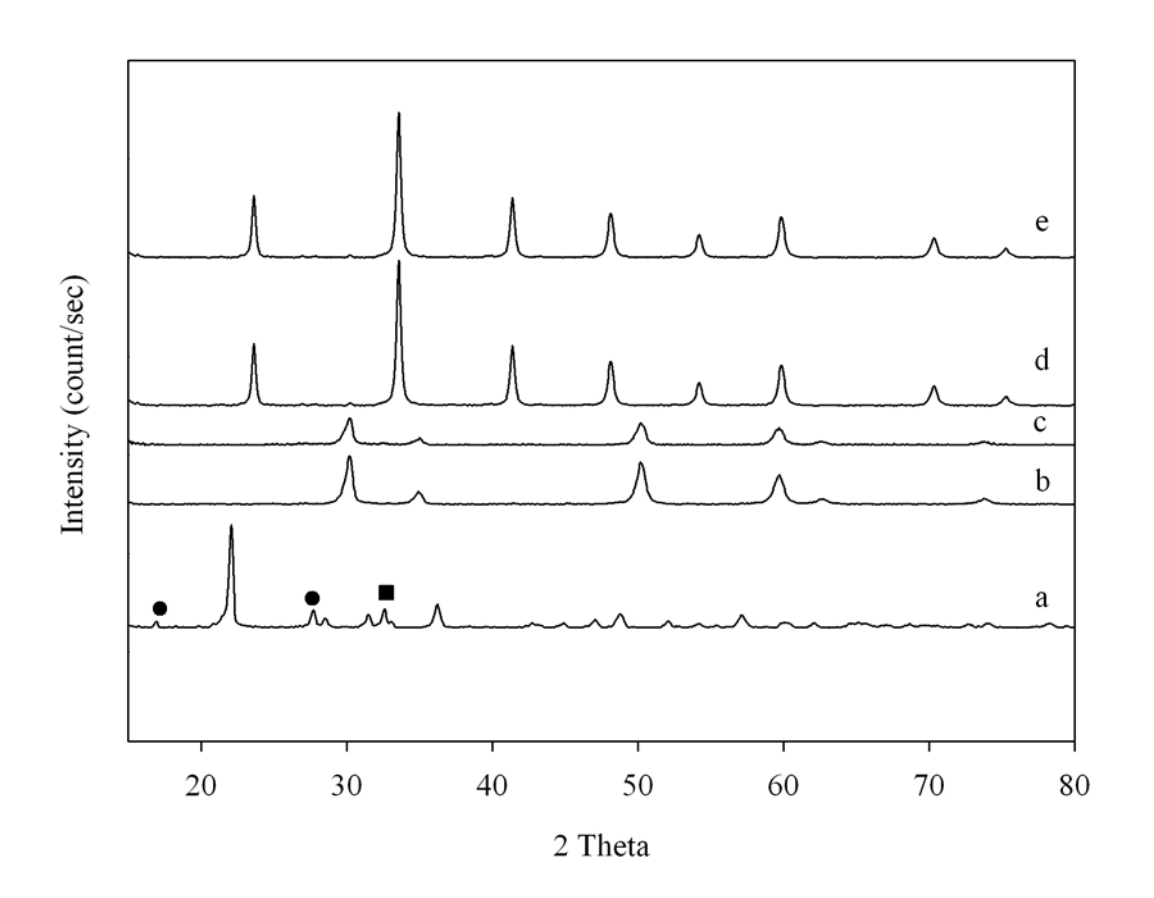


Fig. 5. XRD patterns of (a) Na-W-Mn/SiO $_2$, (b) YSZ, (c) Na-W-Mn/YSZ $_1$ (d) LaAlO $_3$ and (d) Na-W-Mn/LaAlO $_3$. () Na $_2$ WO $_4$, () Mn $_2$ O $_3$

Table 5 Surface composition of fresh catalysts

					O(1s)					
Catalysts	Na(1s)	W(4f)	Mn(2p)	O(1s)	(MO_x)	Si(2p)	Y()	Zr()	La()	Al()
Na-W-Mn/SiO ₂	7.7	0.9	2.8	59.3	16.0	13.2	-	-	-	-
Na-W-Mn/YSZ	12.3	7.2	3.1	24.8	17.8	-	3.8	31.0	-	-
Na-W-										
Mn/LaAlO ₃	8.1	13.0	5.4	5.7	36.7	-	-	-	31.0	-

MO_x represents the metal oxide except SiO₂, ZrO₂ and LaAlO₃

4.6 Catalytic performance of catalysts

Table 6 summarizes the catalytic performances of different catalysts after 90 mins of reaction at steady state under 15000 ml g⁻¹ h⁻¹ of GHSV, 800 °C and a molar ratio of CH₄/O₂ = 4:1. For Na-W-Mn/SiO₂ catalyst, 12.0% CO selectivity, 12.9% CO₂ selectivity and 69.0% C2 selectivity at 28.5% CH₄ conversion is obtained, which is in agreement with several reports. In a comparison among different supports, YSZ shows greater selectivity to partial oxidation than the complete combustion, as the selectivity to CO is much greater than that to CO₂. When Na₂WO₄ and Mn are added on YSZ, the promoting effect of CH₄ conversion has increased from 10.6 to 26.9% and 18.9 to 60.6% for C2 selectivity is obviously observed. It is interesting to note that the promotional tri- metallic oxide (Na₁ W, and Mn) can significantly improve a catalytic performance of YSZ to selective OCM reaction. However, small changes on CH₄ conversion and C2 selectivity are found over LaAlO₃ and Na-W-Mn/LaAlO₃ catalysts (28.8%, 28.0%), whereas C2 selectivity slightly changes from 60.6% to 65.9%.

Effect of temperature for OCM reaction over Na-W-Mn/SiO₂, Na-W-Mn/YSZ and Na-W-Mn/LaAlO₃ catalysts is shown in Fig 6. Trend of CH₄ conversion over three catalysts showed a slightly increase with increasing operating temperature However, decreases in C2 selectivity and C2 hydrocarbon yield are observed in the temperature range of 800-900°C because of kinetic limitations.

The upper limit of OCM yield under conventional fixed bed, continuous feed reactor is considered to be dominated by the enthalpies of hydrogen severance from methane and oxygen dissociative adsorption .The optimum temperature for three catalysts appears at 800°C, where C2 hydrocarbon yields are 19.7%, 16.3% and 18.4% for Na-W-Mn/SiO₂, Na-W-Mn/YSZ and Na-W-Mn/LaAlO₃, respectively in which these results are not significantly different while higher C2 selectivity (75%) is observed over Na-W-Mn/YSZ. A comparison between three catalysts clearly indicates that Na-W-Mn/YSZ is an attractive catalyst for use in SOFC reactor.

Table 6 Catalytic performance of catalysts^a

Catalyst	Conversion (%)	Selectivity (%) Yield (Yield (%)	
	CH ₄	H ₂	СО	CO ₂	C ₂ H ₄	C ₂ H ₆	C ₂	C2
YSZ	10.6	48.5	54.0	27.3	0	18.9	18.9	2.0
LaAlO ₃	28.8	18.7	8.3	27.7	24.7	35.9	60.6	17.4
Na-W-Mn/SiO ₂	28.5	4.1	12.0	12.9	21.2	47.8	69.0	19.7
Na-W-Mn/YSZ	26.9	2.6	9.9	25.2	22.9	37.7	60.6	16.3
Na-W-Mn/LaAlO ₃	28.0	3.6	0.7	28.5	26.3	39.6	65.9	18.4

^a Reaction condition: T=800 $^{\circ}$ C; CH₄/O₂=4; WHSV=15000 mlg $^{-1}$ h $^{-1}$; 0.2 g catalyst.

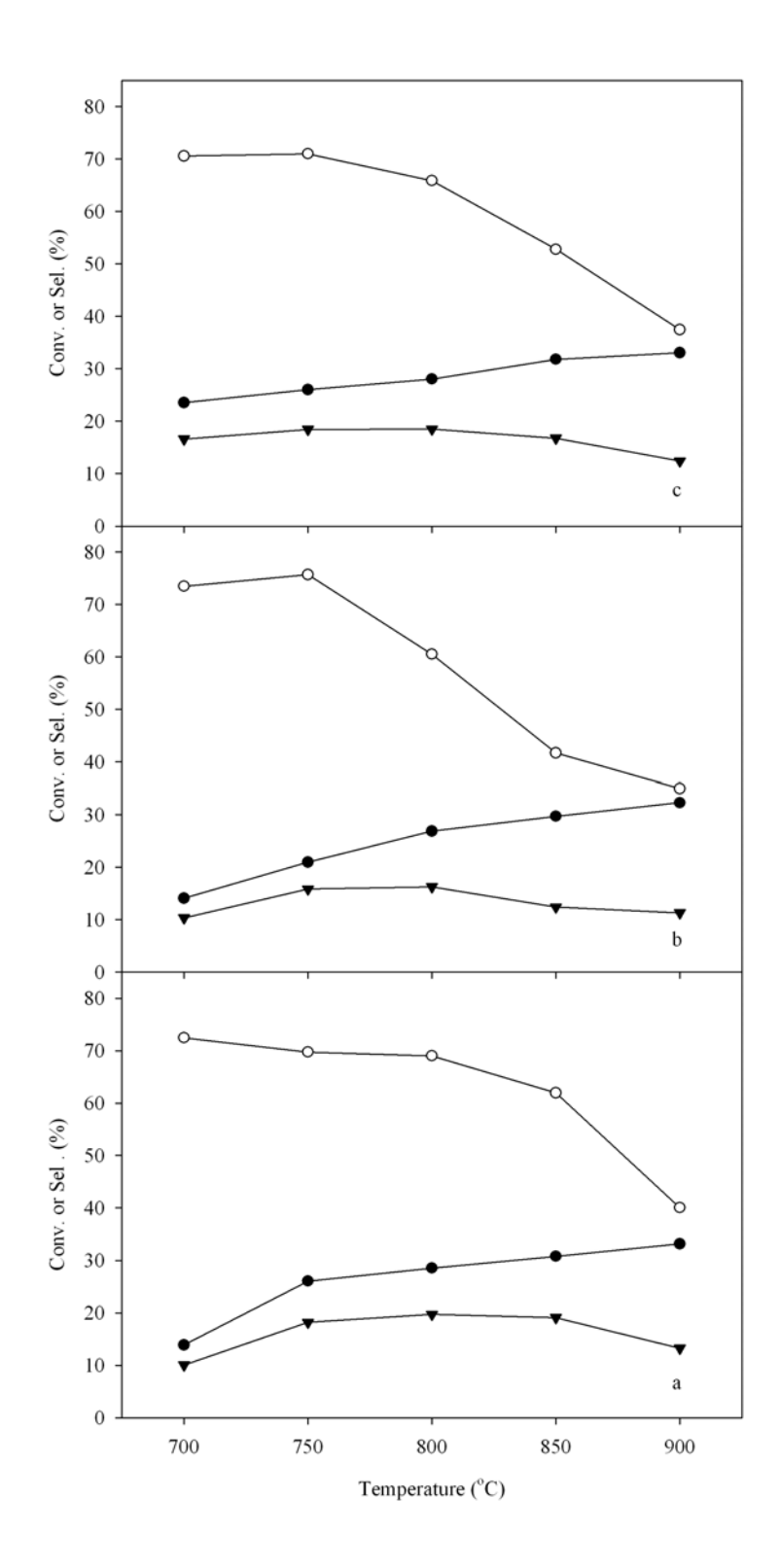


Fig. 6. Catalytic performance of Na-W-Mn/SiO $_2$, Na-W-Mn/YSZ and Na-W-Mn/LaAlO $_3$ catalysts as related to operation temperatures at GHSV of 15000 mlg $^{-1}h^{-1}$ and CH $_4$ /O $_2$ of 4. (a) Na-W-Mn/SiO $_2$, (b) Na-W-Mn/YSZ, (c) Na-W-Mn/LaAlO $_3$. (\bullet) conversion of CH $_4$, (\blacktriangledown) C2 selectivity, (\circ) C2 yield.

4.7 Conclusions

Na-W catalysts supported SiO₂, YSZ and LaAlO₃ catalysts were synthesized, characterized and explored as anode catalyst materials for the OCM reaction. The presence of Mn³⁺ and W⁶⁺ on YSZ are confirmed and they significantly improve a catalytic activity and C2 selectivity despite of a very low surface area YSZ. Additionally, using YSZ as the support can reduce the distance and thickness of interface layer between anode and cathode, resulting in a good diffusion and catalytic reaction. Therefore, Na-W-Mn/YSZ is potentially a promising anode catalyst for use in a SOFC reactor for C2 hydrocarbon production via OCM reaction.

CONCLUSION

5.1 Conclusion

This research work was carried out in order to study the potential use of $Au/La_{0.6}Sr_{0.4}MnO_3$ perovskite materials and Na-W-Mn/YSZ for the oxidative coupling of methane (OCM) reaction. Below are the summaries of these studies:

Reactivity toward Oxidative Coupling of Methane

Au/LSM was synthesised, characterised, and explored as a catalytic material for studying the reaction of methane in fixed bed reactor. It was found that La_{0.6}Sr_{0.4}MnO₃ perovskite was corresponded to characteristic of prepared perovskite. Gold particles that were deposited on perovksite enhanced the catalytic performance such as conversion, selectivity and stability during OCM reaction. Although Au/LSM had a very low surface area, it could significantly improve the catalytic performance. The most attractive Au/LSM nanocomposite had both a high H₂ yield and CO selectivity when operated at a low CH₄/O₂ ratio, whereas greater C2 selectivity was obtained at a higher CH₄:O₂ ratio. It is reasonable that Au/LSM can indeed be used in SOFCs for syngas production or methane oxidative coupling. Thus, Au/LSM catalysts may become a great focus and challenge in the trends of SOFCs.

Na-W catalysts supported SiO_2 , YSZ and LaAlO₃ catalysts were synthesized, characterized and explored as anode catalyst materials for the OCM reaction. The presence of Mn³⁺ and W⁶⁺ on YSZ are confirmed and they significantly improve a catalytic activity and C2 selectivity despite of a very low surface area YSZ. Additionally, using YSZ as the support can reduce the distance and thickness of interface layer between anode and cathode, resulting in a good diffusion and catalytic

reaction. Therefore, Na-W-Mn/YSZ is potentially a promising anode catalyst for use in a SOFC reactor for C2 hydrocarbon production via OCM reaction.

5.2 Suggestion for Future Work

For OCM reaction in SOFC reactor, the conversion of methane and C2 selectivity were obtained very low. Therefore it should be improved and other parameters such as the leak of fuel, loose wire connection, short circuit and crack of cell should be studied. In additional, other operating conditions such as temperature, CH₄:O₂ ratio should be evaluated for increasing C₂ product selectivity and yield.

- [1] J.N. Michaels, C.G. Vayenas, Journal of. Electrochemistry. Society. 131 pp. 2544 ,1984.
- [2] T. Ishihara, T. Yamada, T. Akbay, Y. Takita, Chemistry Engineering. Science. 54 pp. 1535, 1999.
- [3] S. Cimino, G. Landi, L. Lisi, G. Russo, Catalyst Today 11,pp 454, 2006.
- [4] H.J. Wei, Y. Cao, W.J. Ji, C.T., Catalyst Communications. 9, pp.2509, 2008.
- [5] N.U.Pujare, A.F. Sammells, Journal of Electrochemistry Society, 135,pp.2544,1998.
- [6] B.C.H. Steele, A. Heinzel, Nature (London) 414,pp.345,2000.
- [7] B.C.H. Steele, Solid State Ionics 3,p 134, 2000.
- [8] S. Barison, M. Battagliarin, S. Daolio, M. Fabrizio, E. Miorin, P.L. Antonucci, S. Candamano,
 V. Modafferi, E.M. Bauer, C. Bellitto, G. Righini, Solid State Ionics 177,pp. 3473,2007.
- [9] R.M. Navarro, M.C. Alvarez-Galvan, J.A. Villoria, I.D. Gonza´lez-Jime´nez, F. Rosa, J.L.G. Fierro, Applied. Catalysts. B: Environment. 73, pp.247, 2007.
- [10] S. Müllera, K. Striebel, O. Hass, Electrochimica Acta 39, pp. 1661,1994.
- [11] H. Wang, Z. Zhao, P. Liang, C.M. Xu, A.J. Duan, G.Y. Jiang, J. Xu, J. Liu, Catalysts. Letters. 124, pp.91, 2008.
- [12] E.S. Lee, Journal of industry engineering chemistry.14, p.701. 2008.
- [13] M. Haruta, Catalyst Today 36 ,pp. 153,1997.
- [14] M. Haruta, N. Yamada, T. Kobayashi, S. lijima, Journal of catalyst. 115,pp. 30,1989.
- [15] A. Luengnaruemitchai, D.T.K. Thoa, S. Osuwan, E. Gulari, International Hournal of Hydrogen Energy.30 p.981, 2005.
- [16] W.S. Shin, C.R. Jung, J. Han, S.W. Nam, T.H. Lim, S.A. Hong, H.I. Lee, Journal of industry engineering chemistry.10, pp.302, 2004.

- [17] M. Haruta, S. Tsubota, T. Kobayashi, H. Kageyama, M.J. Genet, B. Delmon, Journal Catalysts. 144, pp.175, 1993.
- [18] D.W. Lee, J.H. Ryu, D.H. Jeong, H.S. Lee, K.M. Chun, K.Y. Lee, Journal of industry engineering chemistry, 9, pp.102, 2003.
- [19] A.M. Visco, A. Bonato, C. Milone, S. Galvagno, React. Kinet. Catalysis. letters. 62, p.219, 1997.
- [20] R.D. Waters, J.J. Weimer, J.E. Smith, Catalyst Letters. 30, p.181, 1995.
- [21] H.C. Yang, F.W. Chang, L.S. Roselin, Journal of molecular catalysts A. 276 pp.184, 2007.
- [22] Y.T. Chua, A.R. Mohamed and S. Bhatia, Applied Catalysis A: General, 343 (2008) 142.
- [23] S. Ren, S. Qin, J. Zhu, X. Peng and C. Hu, Industrial and Engineering Chemistry Research, 49 2010 2078.
- [24] J. Wang, L. Chou, B. Zhang, H. Song, J. Zhao, J. Yang and S. Li, Journal of Molecular Catalysis A: Chemical, 245, 2006 272.
- [25] J. Wu, H. Zhang, S. Qin and C. Hu, Applied Catalysis A: General, 323, 2007, 126.
- [26] D. Wang, M.P. Rosynek and J.H. Lunsford, ACS Division of Petroleum Chemistry, Inc. Preprints 1996.
- [27] S. Pak and J.H. Lunsford, Applied Catalysis A: General, 168, 1998,131.
- [28] N. Lapena-Rey and P.H. Middleton, Applied Catalysis A: General, 240 ,2003, 207.
- [29] P. Arora and Z. Zhang, 104, no. 10, pp. 4419-4462, 2004.

- [30] W. Kiatkittipong, Ph.D. dissertation, Department of Chemical Engineering, Chulalongkorn University, Thailand, 2004.
- [31] F. Alcaide, P. L. Cabot, and E. J. Brillas, Journal of Power Sources 153, no. 1, pp. 47-60, 2006.
- [32] K. V. Kordesch and G. R. Simader, Chemical Reviews 95, no. 1, pp.191-207,1996.
- [33] G. F. Mclean, T. Niet, S. Prince-Richard, and N. Djilali, International Journal of Hydrogen Energy, vol.27, no. 5, pp. 507-526, 2002.
- [34] M. Neergat and A. K. Shukla, Journal of Power Sources, 102, no. 1-2, pp. 317-321, 2001.
- [35] A..L.. Dicks, Current Opinion in Solid State and Material Science, 8, no. 5, pp. 379-383, 2004.
- [36] W. Z. Zhu and S. C. Deevi, Material Science and Engineering A,. 362, no. 1-2, pp. 228-239, 2003.
- [37] A. B. Stambouli and E. Traversa, Renewable and Sustainable Energy Review, 6, no. 5, pp. 433–455, 2002.
- [38] O'Hayre, R., Cha, S., Colella, W. and Prinz, F.B. (2006) Fuel Cell Fundamentals, New Jersey, John Wiley & Sons, Inc., pp. 244-246.
- [39] Molenda, J. (2006) High-Temperature Solid-Oxide Fuel Cells: New Trends in Materials Research,

 Materials Science-Poland, 24, (1), pp. 5-11
- [40] EG&G Technical Services, Inc. (2004) Fuel Cell Handbook, 7th Ed., West Virginia., U.S. Department of Energy, pp. (1-1)-(1-32), (7-1)-(7-45).
- [41] McIntosh, S. and Gorte, R.J. (2004), Chemical Reviews, 104, pp. 4845-4865.
- [42] R. D. Farr and C. G. Vayenas,, Journal of Electrochemical Society, vol. 127, no. 7, pp.1478-1483, 1980.
- [43] N. Kiratzis and M. Stoukides, Journal of Electrochemical Society, 134, no.8, pp.1925-1929, 1987.

- [44] E. A. McKenna, A. Othoneos, N. Kiratzis, and M. Stoukides, Journal of Electrochemical Society, 134. no. 8, pp. 1925-1929, 1987.
- [45] J. N. Michaels and C. G. Vayenas, Journal of Electrochemical Society, 131, no. 11, pp. 2544-2550, 1984.
- [46] B. Ji, J. Wang, W. Chu, W. Yang and L. LinB., Chemistry Communication., 21, pp. 2038-2040, 2009.
- [47] S. Neophytides and C. G. Vayenas, Journal of Electrochemistry Society, 137, no. 3, pp. 839-845, 1990.
- [48] I. V. Yentekakis and C. G. Vayenas, Journal of The Electrochemical Society, 136, no. 4, pp. 996-1002, 1989.
- [49] J. A. Hugill, F. W. A. Tillemans, J. W. Dijkstra, and S. Spoelstra, Applied Thermal Engineering, 25, no. 8-9, pp. 1259-1271, 2005.
- [50] H. Zhang, J. Wu, B. Xu, and C. Hu, Catalysis Letters, 106, no. 3-4, pp.161-165, 2006.
- [51] R. A. Periana, O. Mironov, D. Taube, G. Bhalla, and C. J. Jones, Topics in Catalysis, 32, no. 3-4, pp. 169-174, 2005.
- [52] J. Wang, L. Chou, B. Zhang, H. Song, J. Zhao, J. Yang, and S. Li, Journal of Molecular Catalysis A: Chemical, 245, no. 1-2, pp. 272- 277, 2006.
- [53] N. A. S. Amin and S. E. Pheng, Chemical Engineering Journal, 116, no. 3, pp. 187-195, 2006.
- [54] N. U. Pujare and A. F. Sammells, Journal of Electrochemical Society, 135, no. 10, pp. 2544-2545, 1988.
- [55] K. Otsuka, K. Suga, and I. Yamanaka, Catalysis Today, 6, no. 4, pp. 587-592,1990.
- [56] Y. Jiang, I. V. Yentekakis, and C. G. Vayenas, Science, 264, no. 5165, pp. 1563-1566, 1994
- [57] X. M. Guo, K, Hidajat, and C. B. Ching, Korean Journal of Chemical Engineering, vol. 15, no. 5, pp. 469-473,1998.

- [58] W. Kiatkittipong, S. Goto, T. Tagawa, S. Assabumrungrat, and P. Praserthdam, Journal of Chemical Engineering of Japan, 38, no. 10, pp. 841- 848, 2005.
- [59] V. V. Galvita, V. D. Belyaev, A. K. Demin, and V. A. Sobyanin, Applied Catalysis A: General, 165, no. 1-2, pp. 301-308, 1997.
- [60] T. Yamada, Y. Hiei, T. Akbay, T. Ishihara, and Y. Takita, Solid State Ionics, 113–115, no. 11, pp. 253–258, 1998.
- [61] V. A. Sobyanin and V. D. Belyaev, Solid State Ionics, 136-137, pp. 747-752, 2000.
- [62] H. E. Vollmar, C. U. Maier, C. Nolscher, T. Merclein, and M. Poppinger,86, no. 1-2, pp. 90-97, 2000.
- [63] X. Zhang, S. Ohara, H. Chen, and T. Fukui, Fuel, 81, no. 8, pp. 989-996, 2002.
- [64] Z. Zhan, Y. Lin, M. Pillai, I. Kim, and S. A. Barnett, Journal of Power Sources,161, no. 1, pp. 460-465, 2006.
- [65] T. J. Huang and M. C. Huang, Journal of Power Sources ,175, no.1, pp. 473-481, 2008.
- [66] T. J. Huang and M. C. Huang, Chemical Engineering Journal, 135, no. 3, pp.216-223, 2008.
- [67] T. J. Huang and M. C. Huang, Chemical Engineering Journal, 138, no. 1-3, pp. 538-547, 2008.
- [68] T. J. Huang and M. C. Huang, Journal of Power Sources, 168, no. 1, pp. 229-235, 2007.
- [69] T. J. Huang and M. C. Huang, "International Journal of Hydrogen Energy, vol. 34, no. 6, pp. 2731-2738, 2009.
- [70] T. Ishihara, T. Yamada, T. Akbay, and Y. Takita, Chemical Engineering Science, 54, no. 10, pp. 1535-1540,1999.
- [71] M. R. Pillai, D. M. Bierschenk, and S. A. Barnett, Catalysis Letter, 121, no. 1-2, pp.19-23, 2007.
- [72] F. Paloukis and S. G. Neophytides, Chemical Engineering Science, 62, no.15, pp. 3868-3881, 2007.
- [73] T. Brousas, P. H. Chiang, D. Eng and M. Stoukides, Ionics, 1, no. 4, pp. 328-337, 1995.

- [74] C. G. Vayenas, S. I. Bebelis, and C. C. Kyriazis, Chemtech, 21, no. 7, pp. 422-428, 1991.
- [75] Twu, J. and Gallagher, P.K. (1993), New York, Marcel Dekker, Inc., pp. 1-23.
- [76] Peña, M.A. and Fierro, J.L.G., 101, pp. 1981-2017. 2001.
- [77] Lok, M.Wiley-VCH., pp. 135-145, 2009.
- [78] Louis, C., Synthesis of Solid Catalyst, Weinheim, In: Krijn, P. de Jong ed., Wiley–VCH., pp. 369-388, 2009.
- [79] G.E. Keller and M.M. Bhasin, Journal of Catalysis, 73, pp. 9-19, 1982.
- [80] M.M Mench, Fuel Cell Engines, John Wiley & Sons, ING., 2008.
- [81] V.R. Choundhary and V.H. Rane, Catalysis Letters, 16,,pp211-215,1992.
- [82] G.E. Keller and M.M. Bhasin, Journal of Catalysis, 73, p. 9-19,1982.
- [83] X.P. Fang, S.B. Li, J.Z. and Y.L. Chu, Journal of Molecular Catalysis (china),6,pp 427-433, 1992.
- [84] D.J. Wang, M.P. Rosynek and J.H. Lunsford, Journal of catalysis, 115, pp. 390-402, 1995.
- [85] J.E. Ten Elshof, B.A. Vanhassel and H.J.M. Bouwmeester, Catalysis Today, 1995, 25, pp. 397–402.
- [86] K. Otsuka, K. Suga and I. Yamanaka, Catalysis. Letters, 1, pp. 423,1998.
- [87] K. Otsuka, K. Suga and I. Yamanaka, I. Chemistry Letters,pp. 317,1998
- [88] A. G. Andersen, T. Hayakawa, K. Suzuki, M. Shimizu and K. Takehira, Catalysis Letters, 27, pp. 221-223,1994.
- [89] X.M. Guo, K. Hidajat and C.B. Ching, Journal of Industry Engineering, Chemistry. Resource., 36, pp. 3576-3582,1997.
- [90] M. Gaudon, C.L. Robert, F. Ansart, P. Stevens, A. Rousset, Solid State Sci. 4 pp.125, 2002.
- [91] J. Nui, J. Deng, W. Liu, L. Zhang, G. Wang, H. Dai, H. He, X. Zi, Cataysis. Today, 126, pp. 420, 2007.

- [92] S. Daengskul, C. Thomas, I. Thomas, C. Mongkolkachit, S. Siri, V. Amornkibamrung, S. Maensiri, Nanoscale Resource Letters 4,pp.839, 2009.
- [93] A. Luengnaruemitchai, D.T.K. Thoa, S. Osuwan, E. Gulari, Int. J. Hydrogen Energy 30, pp.981, 2005.
- [94] T. Sreethawong, S. Yoshikawa, Catalysis Communication, 6, pp.661, 2005.
- [95] F.W.Chang, H.Y. Yu, L.S. Roselin, H.C. Yang, Applied Catalysis A: 290, pp. 138, 2005.
- [96] A. Malekzadeh, A. Khodadadi, A.K. Dalai and M. Abedini, Oxidative Coupling of Methane over Lithium Doped (Mn⁺W)/SiO₂ Catalysts, Journal of Natural Gas Chemistry, 16,121, 2007.

OUTPUT

International Journal Publication

1. **Wiyaratn W**, Appamana W, Sumittra Charojrochkul Sitichai Kaewkuekool Assabumrungrat S, Au/La_{1-x}Sr_xMnO₃ nanocomposite for chemical-energy cogeneration in solid oxide fuel cell reactor. *Journal of Industrial and Engineering Chemistry* 2012. **(Published)** (Impact factor- 2012= 2.145)

International conference

1. Hattachai Aeowjaroenlap, Suttichai Assabumrungrat, **Wisitsree Wiyaratn**, Simulation of the oxidative coupling of methane process for C2 production from biomass. Pure and Applied Chemistry International Conference (PACCON 2014), 8-10 Januray, 2014, Thailand

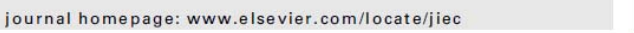
ภาคผนวก

Journal of Industrial and Engineering Chemistry 18 (2012) 1819-1823



Contents lists available at SciVerse ScienceDirect

Journal of Industrial and Engineering Chemistry





Au/La_{1-x}Sr_xMnO₃ nanocomposite for chemical-energy cogeneration in solid oxide fuel cell reactor

Wisitsree Wiyaratn ^{a,*}, Weerinda Appamana ^b, Sumittra Charojrochkul ^c, Sittichai Kaewkuekool ^a, Suttichai Assabumrungrat ^b

^a Department of Production Technology and Education, Faculty of Industrial Education and Technology, King Mongkut's University of Technology Thonburi, Bangkok 10140, Thailand ^bCentre of Excellence in Catalysis and Catalytic Reaction Engineering, Department of Chemical Engineering, Faculty of Engineering, Chulalongkom University, Ranghold 1030 Thoilmal

Bangkok 10330, Thailand ^cNational Metal and Materials Technology Center (MTEC), Pathumthani 12120, Thailand

ARTICLE INFO

Article history: Received 10 October 2011 Accepted 15 April 2012 Available online 21 April 2012

Keywords: SOFC reactor Cogeneration Au/La_{1-x}Sr_xMnO₃ nanocomposite C₂ hydrocarbon

ABSTRACT

Au/La_{1-x}Sr_xMnO₃ ($x\approx0.4$, Au/LSM) nanocomposites were synthesised and investigated for their potential use in an oxidative coupling of methane (OCM) reaction in a fixed bed reactor (FBR) and solid oxide fuel cell reactor (SOFC). A 17.9% C₂ selectivity and a 10.8% CH₄ conversion have been obtained in a FBR at 1073 K and 6:1 CH₄/O₂. The electron motive force was 0.86 V at the power density of 12.4 mA cm⁻² during cogeneration through OCM in SOFC reactor. A 7% methane conversion and a 5.7% C₂ selectivity were obtained when the air flow rate was 30 ml/min at 1123 K.

© 2012 The Korean Society of Industrial and Engineering Chemistry. Published by Elsevier B.V. All rights

SIMULATION OF THE OXIDATIVE COUPLING OF METHANE PROCESS FOR C2 PRODUCTION FROM BIOMASS

Hattachai Aeowjaroenlap¹, Suttichai Assabumrungrat¹, Wisitsree Wiyaratn²,

¹ Department of Chemical Engineering, Faculty of Engineering, Chulalongkorn University, Bangkok, 10330, Thailand ² Faculty of Industrial Education and Technology, King Monkut's University of Technology Thonburi, Bangkok, 10140, Thailand

Abstract: In this study, the process model for C2 production from biomass was developed and simulated by ASPEN PLUS program. Plant capacity was designed at 200,000 tons of biomass per year (dry basis). Wheat straw was considered as raw material which was reduced in size as a preliminary treatment before pretreated by two-step steam explosion at 100oC and 180oC and then fed to produce biogas by solid state digestion method. Biogas was subsequently fed to produce C2 via the oxidative coupling of methane over Na-W-Mn/SiO2 catalyst at 850oC and 1 atm. The model results showed that wheat straw can be converted to ethane and ethylene, which were the main building block for petrochemical industry.

1. Introduction

Nowadays, the production of chemicals from biomass obtains more attraction as one of the most primary alternatives for sustainable development. Production of biogas, which consists mainly of methane, from industrial or municipal wastes becomes an appropriate way to replace the usage of methane from natural gas. Use of lignocellulosic biomass, such as wheat straw, has more advantage than sugar or starch derivatives in case of availability and prices. But, the limitation of crystallinity and stability structure of lignocellulose requires pretreatment step such as steam explosion to open crystalline structure and prepare for an anaerobic digestion [1].

Biogas, which is mainly of methane, can be an alternative fuel source instead of fossil fuel. However, use of methane as raw materials to synthesis higher valuable hydrocarbons is a promising way to reduce the usage of petroleum feedstock. Methane conversion process is including Fischer-Tropsch synthesis, partial oxidation to methanol and the oxidative coupling of methane (OCM).

Ethane and ethylene are now conventionally produced by the cracking process of higher hydrocarbons feedstock such as naphtha, which is a derivative of the fossil fuel. However, production of C2 hydrocarbons, especially ethane and ethylene, from the oxidative coupling of methane, receives more attention from researchers during the last decade. Many effective catalysts for the oxidative coupling of methane have been reported. Na₂WO₄/Mn/SiO₂ (Na-W-Mn/SiO₂) is known as one of the most effective catalyst for OCM reaction due to its good catalytic activity, selectivity and also a thermal stability.

Comprehensive kinetic model of OCM over Na-W-Mn/SiO2, which contains nine heterogeneous reactions on catalyst surface and one homogeneous gas phase reaction, is reported by M. Daneshpayeh et al. [2]. The reaction network is described below;

$$\begin{array}{c} CH_4 + 2O_2 \rightarrow CO_2 + H_2O & (1) \\ 2CH_4 + 0.5O_2 \rightarrow C_2H_6 + H_2O & (2) \\ CH_4 + O_2 \rightarrow CO + H_2O + H_2 & (3) \\ CO + 0.5O_2 \rightarrow CO_2 & (4) \\ C_2H_6 + 0.5O_2 \rightarrow C_2H_4 + H_2O & (5) \\ C_2H_4 + 2O_2 \rightarrow 2CO + 2H_2O & (6) \\ C_2H_6 \rightarrow C_2H_4 + H_2 & (7) \\ C_2H_4 + 2H_2O \rightarrow 2CO + 4H_4 & (8) \\ CO + H_2O \rightarrow CO_2 + H_2 & (9) \\ CO_2 + H_2 \rightarrow CO + H_2O & (10) \end{array}$$

In this study, C2 hydrocarbons (ethane and ethylene) production process via the oxidative coupling of methane from wheat straw was designed and simulated in Aspen Plus program with plant capacity of 200 kton per year of wheat straw feed. The kinetic model of OCM over Na-W-Mn/SiO2 proposed by M. Daneshpayeh was employed in the rigorous RPlug reactor model.

2. Simulation

Process simulation of OCM for C2 production from biomass was executed by using Aspen Plus program. Biogas production process from wheat straw proposed by M. Shafiei et al. [1] and carbon dioxide removal by chemical absorption of monoethanolamine (MEA) solvent [3-5] were applied in this study. The Electrolyte Non-Random Two Liquid Activity Coefficient model (ELECNRTL) was used in the simulation because of the electrolytic property of CO2-MEA-H2O mixture system.

The entire process was divided into four sections including biogas production, biogas treatment, OCM reaction and product separation.

2.1 Biogas production from wheat straw

M. Shafiei et al. [1] proposed a novel process that converted the wheat straw to biogas at the capacity of 200 kton per year (dry basis). The aforementioned process of biogas production, shown in figure 1, was employed in this study.

^{*}Author for correspondence; wisitsree.wiy@kmutt.ac.th, Tel. +66 2470 8554

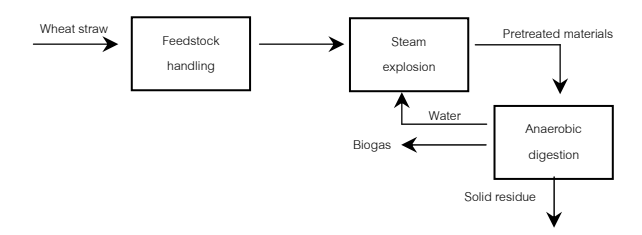


Figure 1: Simplified block flow diagram for biogas production from wheat straw as biomass by the steam explosion and anaerobic digestion

2.2 Removal of carbon dioxide from biogas

Biogas produced from anaerobic digestion process consisted of a significant amount of carbon dioxide which is the cause of lower activity of reaction and increase of gas loading for the later of the process; therefore, the amine absorption process by 30 wt% MEA solvent was used to remove carbon dioxide in gas mixture to reach more than 90 mole% of methane purity. After carbon dioxide was absorbed, water content in gas stream was then reduced by the condenser.

Process flow diagram for this section was depicted in figure 2 and the list of unit operation was summarized in table 1.

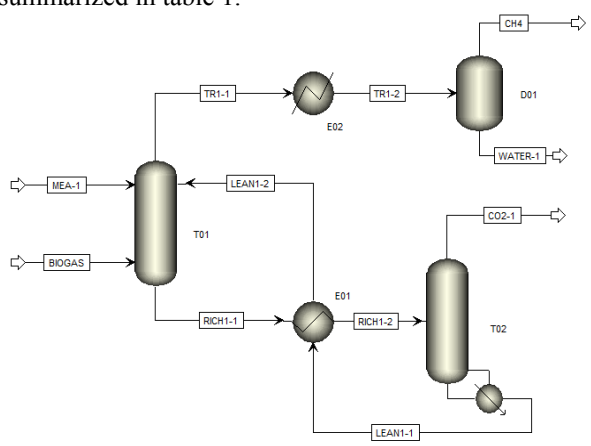


Figure 2: Process flow diagram for biogas treatment section

Table 1: Unit operation in biogas treatment section

T01 Absorber	
Packing height	12 m
Packing diameter	2 m
Packing type	IMTP #40
Pressure (atm)	0.987
T02 Stripper	
No. of stages	20
Molar boilup ratio	0.1
Pressure (kPa)	101.43
Pressure drop (kPa)	1.895
E02 Cooler	
Outlet temperature (°C)	30

2.3 Oxidative coupling of methane section

Methane from biogas was consequently fed together with oxygen and methane recycle stream to the heat exchanger which temperature of gas stream was raised to 850°C with the control pressure of 1 atm. In the rigorous isothermal RPlug reactor, the OCM reaction network took place over the Na-W-Mn/SiO2 catalyst. After the reactor, the effluent was cooled down to 30°C before fed to the product separation section.

Process flow diagram for this section was shown in figure 3 and the list of unit operation was summarized in table 2.

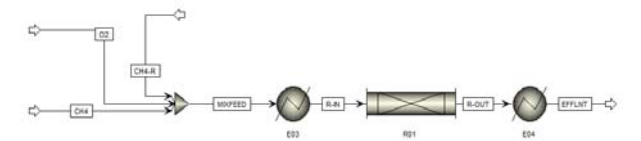


Figure 3: Process flow diagram for oxidative coupling of methane section

Table 2: Unit operation in OCM section

E03 Heater	
Outlet temperature (°C)	850
R01 Packed bed reactor	
Temperature (°C)	850
Bed voidage	0.45
Cat. particle density (kg/m ³)	1100
E04 Cooler	
Outlet temp. (°C)	30

2.4 Product separation section

Effluent from OCM reactor consisted of unreacted methane, ethane, ethylene, carbon monoxide, carbon dioxide, oxygen and water. Ethane and ethylene should be separated from other components in order to meet the requirement of downstream process. Firstly, carbon dioxide was removed by MEA absorption followed by the removal of water by compressed-condensation at high pressure. Methane and mixed C2 hydrocarbons were separated by distillation column with partial condenser. 80-95% of unreacted methane together with other components was recycled to the OCM reactor while the remaining was purged from the process.

Process flow diagram for this section was shown in figure 4 and the list of unit operation was summarized in table 3.

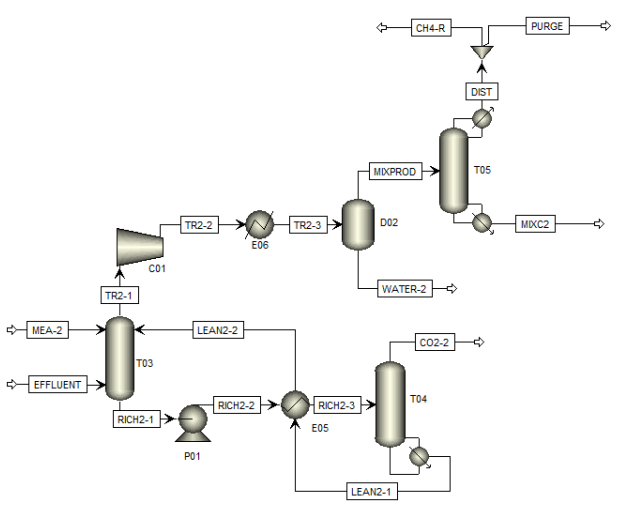


Figure 4: Process flow diagram for product separation section

Table 3: Unit operation in product separation section

T03 Absorber	
Packing height	18 m
Packing diameter	3 m
Packing type	IMTP #40
Pressure (kPa)	100
T04 Stripper	
No. of stages	20
Molar boilup ratio	0.1
Pressure (kPa)	101.43
Pressure drop (kPa)	1.895
C02 Gas compressor	
Outlet pressure. (MPa)	1.013
E06 Cooler	
Outlet temperature (°C)	30
T05 Distillation column	
Pressure (MPa)	1.013
No. of stage	14
Molar reflux ratio	0.211
Distillate to feed fraction	0.837

2.5 Effect CH4-R stream recycle flow rate on the heat duty of overall process and C2 yields

To overcome the limitation of low methane conversion for OCM reactor, the unreacted methane should be recycled so as to obtain more C2 yields, selectivity and methane conversion. The %Recycle and C2 yields [6] were defined as follow:

% Recycle =
$$\frac{\text{Flow rate of } CH4-R}{\text{Flow rate of } DIST} \times 100 \tag{11}$$
% C2 yields =
$$\frac{\Box \text{ (n x moles of C}_n \text{ in products)}}{\text{moles of } CH_a \text{ in feed}} \times 100 \tag{12}$$

The basecase %Recycle was set to 90%, to study effect of %Recycle, %Recycle was varied from 80% to 95%.

3. Results and Discussion

3.1 Biogas production from biomass

From M. Shafiei et al.'s work, components that consisted in wheat straw, which were used in simulation, were hexosan, pentosan, lignin and water. After wheat straw was pretreated by 2-step steam explosion (LP steam at 100oC and HP steam at 180oC), those components were digested by anaerobic digestor and then, methane and carbon dioxide were produced. Raw materials and product input-output of the process was proposed as table 4.

Table 4: Raw material feed and product distribution of the biogas production process

Component	Biomass	Biogas
Mass frac.	(Raw mat.)	(Product)
Water	0.150	0.095
Hexosan	0.432	=
Pentosan	0.229	-
Lignin	0.198	-
Methane	ı	0.242
CO_2	-	0.663
Total (kton/year)	235.3	172.5

3.2 OCM plant input-output information

Biogas from previous section was served as raw material for OCM process. From simulation study, components which were fed and were generated from the process were summarized in Feed and Output as reported in table 5.

Table 5: Components feed and output of the OCM reaction section

Component	Feed	Output		
Component	(kmol/hr)	kmol/hr	kg/hr	
Methane	270	56	896	
Oxygen	140	-	-	
Ethane	-	34	1020	
Ethylene	-	48	1346	
Carbon monoxide	-	2	56	
Carbon dioxide	17	134	5896	
Water	13	393	7074	
Total	300	673	16288	

As shown in table 5, 1020 kilograms per hour of ethane and 1346 kilograms per hour of ethylene were produced respectively. C2 yield was 60.7% at %Recycle of 90%.

Due to high reaction temperature, reaction pathway of methane is favor to the complete combustion which resulted in generation of carbon dioxide and water instead of the OCM. Therefore, supplying of oxygen to the reactor must be controlled to prevent the unwanted complete combustion of methane. So, there were significant amount of methane remaining from the reaction which needed to be recycled.

3.3 Energy requirement of the process

Energy requirement calculated from the unit operation in the process i.e. heat exchangers, reactor, pumps and compressor, was summarized in table 6. Note that the duty was reported in absolute value.

Table 6: Components feed and output of the OCM reaction section

Unit operation	Duty (kW)
T02 (Reboiler)	4275
E02 (Cooler)	4270
E03 (Heater)	12667
R01(Reactor)	14418
E04 (Cooler)	14098
P01 (Pump)	negligible
T04 (Reboiler)	993
C01 (Compressor)	2398
E06 (Cooler)	3785
T05 (Condensor)	367
T05 (Reboiler)	939
Total	58210

Total energy requirement for OCM process was 58210 kW (58.21 MW) at %Recycle of 90%.

From figure 4, major of process duty should be in the reaction section and the downstream section due to the huge amount of gas flow rate in the process. That was confirmed by results showed in table 6.

3.4 Effect of unreacted CH4 recycle flow rate on the heat duty of overall process and C2 yields

From simulation study, %Recycle of CH4-R stream was varied from 85% to 95% respectively. The results were displayed in figure 5.

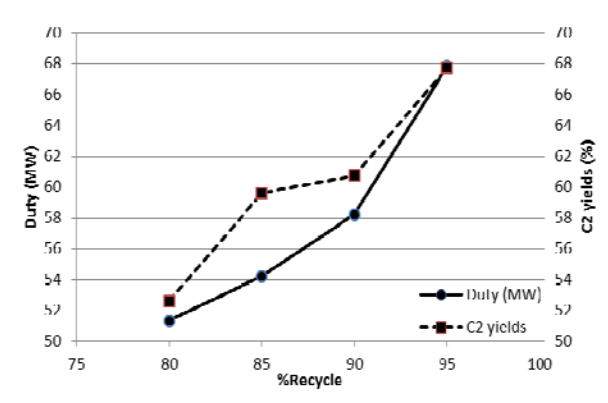


Figure 5: Effect of %Recycle on process duty and C2 yields

In case of maximizing product output (for more C2 products obtained), unreacted methane should be recycled as much as possible. But, however, increasing

of %Recycle resulted in increasing of process duty as shown in figure 5. Therefore, in order to justify the economic of this process, the economical point of view should be further investigated.

4. Conclusion

In this study, C2 (ethane and ethylene) production process from biomass was designed and simulated in Aspen Plus program. The results showed that 200 kton per year of wheat straw could be converted to 4320 kilograms of methane per hour which converted to 2366 kilograms per hour of C2 product. The process duty was 58.21 MW at 90%Reclycle of CH4-R stream. However, in case of process economy, more information about investment cost and operating cost should be taken into account.

Acknowledgement

The authors gratefully acknowledge the Thailand Research Fund and Higher Education Commission, and King Mongkut's University of Technology Thonburi for financial support.

References

- [1] Shafiei M., Kabir M.M., Zilouei H., Horváth I.S and Karimi K., *Techno-economical study of biogas production improved by steam explosion pretreatment.* Bioresource Technology, 2013. **148**: p. 53-60.
- [2] Daneshpayeh M., Khodadadi A., Mostoufi N. and Mortazavi Y., Kinetic modeling of oxidative coupling of methane over Mn/Na₂WO₄/SiO₂ catalyst. Fuel Processing Technology, 2009. 90: p.403-410.
- [3] Aspen Plus, Example for rate-based model of the CO₂ capture process by MEA using Aspen Plus. Aspen Technology, Inc., 2008.
- [4] Moioli S., Pellegrini L. A., Gamba S., Simulation of CO₂ capture by MEA scrubbing with a rate-based model. Procedia Engineering, 2012. 42: p. 1651-166
- [5] Zhang M.,Guo Y., Process simulations of large-scale CO₂ capture in coal-fired power plants using aqueous ammonia solution. International Journal of Greenhouse Gas Control, 2013. 16: p. 61-71
- [6] Chua Y.T., Mohamed A.R., Bhatia S., Oxidative coupling of methane for the production of ethylene over sodium-tungsten-manganese-supported-silica catalyst (Na-W-Mn/SiO₂). Applied Catalysis A: General, 2008. **343**: p. 142-148



CHULA ENGINEERING

Foundation toward Innovation



SIMULATION OF THE OXIDATIVE COUPLING OF METHANE PROCESS FOR C2 PRODUCTION FROM BIOMASS

Hattachai Aeowjaroenlap¹, Suttichai Assabumrungrat¹, Wisitsree Wiyaratn²,

¹ Department of Chemical Engineering, Faculty of Engineering, Chulalongkorn University, Bangkok, 10330, Thailand ² Faculty of Industrial Education and Technology, King Monkut's University of Technology Thonburi, Bangkok, 10140, Thailand

*Author for correspondence; E-mail: wisitsree.wiy@kmutt.ac.th, Tel. +66 2470 8554

Abstract

In this study, the process model for C_2 production from biomass was developed and simulated by ASPEN PLUS program. Plant capacity was designed at 200,000 tons of biomass per year (dry basis). Wheat straw was considered as row material which was reduced in size as a preliminary treatment before pretreated by two-step steam explosion at $100^{\circ}C$ and $180^{\circ}C$ and then fed to produce biogas by solid state digestion method. Biogas was subsequently fed to produce C_2 via the oxidative coupling of methone (QCM) over Na-W-Mn/SiQ₂ catalyst at $850^{\circ}C$ and 1 atm. The model results showed that wheat straw can be converted to ethane and ethylene successfully, which were the main building block for petrochemical industry.

Introduction



- To reduce the consumption rate of petroleum and reduce the amount of CO₂ in atmosphere, biogas has received much attention to use as raw materials to synthesis higher HCs.
- Wheat straw was used as biomass feedstock, at 200 ktons annually, to produce biogas [1].

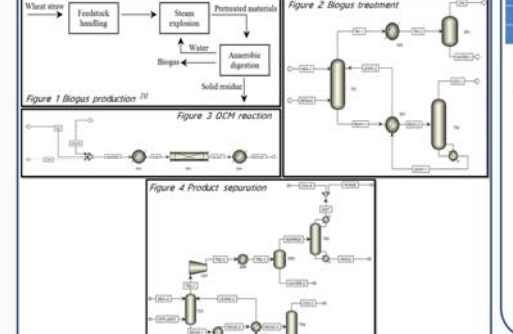


 Biogas was supplied to the OCM Process which have the following reaction network over Na-W-Mn/SiO₂ catalyst [2].

$CH_4+2O_2 \rightarrow CO_2 + H_2O$	(1)	$C_2H_4 + 2O_2 \rightarrow 2CO + 2H_2O$	(6)
$2CH_4 + 0.50_2 \rightarrow C_2H_6 + H_2O$	(2)	$C_2H_6 \rightarrow C_2H_4 + H_2$	(7)
$CH_4 + O_2 \rightarrow CO + H_2O + H_2$	(3)	$C_2H_4 + 2H_2O \rightarrow 2CO + 4H_4$	(8)
$CO + 0.50_2 \rightarrow CO_2$	(4)	$CO + H_2O \rightarrow CO_2 + H_2$	(9)
$C_2H_6 + 0.50_2 \rightarrow C_2H_4 + H_2O$	(5)	$CO_2 + H_2 \rightarrow CO + H_2O$	(10)

Simulation

 Process was simulated by ASPEN Plus program with ELEC-NRTL property method. The entire process was divided into four sections including biogas production, biogas treatment, OCM reaction and product separation as shown in figure 1-4.



- Process model included rigorous plug flow reactor (RPlug), MEA scrubbing for CO₂ removal (RateSep for absorber and RadFrac for stripper[3-5]) and distillation column for methane-mixed C₂ separation.
- Effect CH4-R stream recycle flow rate on the heat duty of overall process and C2 yields [6].

 $\% \text{Recycle} = \frac{\text{Flow rate of } CH4\text{-}R}{\text{Flow rate of } DIST} \times 100$ $\% \text{C}_2 \text{ yields} = \frac{\sum (\text{n x moles of Ch4 in freed})}{\text{moles of CH4 in feed}} \times 100$

Results and Discussion

Table 1: Raw material feed and product distribution of the biogas production

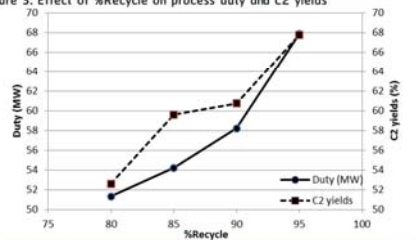
Mass frac.	(Raw mat.)	Biogas (Product)	
Water	0.150	0.095	
Hexoson	0.432		
Pentosan	0.229	-	
Lignin	0.198	120	
Hethane	-	0.242	
CO2	-	0.663	
Total (kton/year)	235.3	172.5	

Table 2: Components feed and output of the OCM process section including

process duty required

Component Feed (kmol/hr)	Feed	Output		Unit operation	Duty (kW)
	kmol/hr	kg/hr			
Methane	270	56	896	TO2 (Reboiler)	4275
Oxygen	140			E02 (Cooler)	4270
Ethane	-	34	1020	E03 (Heater)	12667
Ethylene	-	48	1346	R01(Reactor)	14418
Carbon		- z	56	E04 (Cooler)	14098
monoxide				P01 (Pump)	negligible
Carbon		134	5896	T04 (Reboiler)	993
dioxide	17			CO1 (Compressor)	2398
Water	13	393	7074	E06 (Cooler)	3785
Total	300	673	16288	TOS (Condensor)	367
				TOS (Reboiler)	939
				Total	58210

Figure S: Effect of %Recycle on process duty and C2 yields



Conclusion

 $\rm C_2$ (ethane and ethylene) production process from biomass was designed and simulated by Aspen Plus program. Wheat straw 200 kton per year could be converted to 4320 kg/h of methane which converted to 2366 kg/h of $\rm C_2$ product. The process duty was 58.21 MW at 90%Rectycle of *CH4-R* stream. To justify the process economy, more information about investment cost and operating cost should be taken into account.

[1] Stude M., Kalar M.P., Zhous M., Navride N.S. vol Karmi K., Bohne-parametric disk of Inique production improve for drawn equivalen personner Berbrings, 2011. 148 g. 53-60.
[2] Developping M., Orderfell B., Mitsmall K., and Mitsmallar M. - Profess continger of continue and evidence or in Principle (Sylv), control or fair informing behaviors, 2011. 159 at 40-40.
[2] Dissame Principle M. - Development or through and control of the Collision and principle (Sylv), control or fair informing behaviors, 2011. 159 at 40-40.
[3] Dissame Principle M. - Development or through and control or the Collision and Collision a